

This is the accepted manuscript prior to copyediting and page composition (post-print). The publisher's version can be accessed at:

<http://www.nrcresearchpress.com/doi/abs/10.1139/cjfas-2016-0376>

1 **Validation of a hidden Markov model for the geolocation of Atlantic**  
2 **cod**

3 **CHANG LIU<sup>1</sup>, GEOFFREY W. COWLES<sup>1</sup>, DOUGLAS R. ZEMECKIS<sup>1, \*</sup>, STEVEN**  
4 **X. CADRIN<sup>1</sup>, AND MICAH J. DEAN<sup>2</sup>**

5 *<sup>1</sup>Department of Fisheries Oceanography*

6 *School for Marine Science and Technology*

7 *University of Massachusetts Dartmouth*

8 *706 S Rodney French Blvd, New Bedford, MA 02744, USA*

9 *<sup>2</sup>Annisquam River Marine Fisheries Field Station*

10 *Massachusetts Division of Marine Fisheries*

11 *30 Emerson Ave., Gloucester, MA 01930, USA*

12 Corresponding author: Chang Liu, cliu3@umassd.edu

13 \*Present address: Department of Marine and Coastal Sciences, Rutgers University, 71 Dudley  
14 Road, New Brunswick, NJ 08901

## 15 **Abstract**

16 Models developed to geolocate individual fish from data recorded by electronic tags often  
17 require significant modification to be applied to new regions, species, or tag types due to  
18 variability in oceanographic conditions, fish behavior, and data resolution. We developed  
19 a model for geolocating Atlantic cod off New England that builds upon an existing hidden  
20 Markov model (HMM) framework and addresses region- and species-specific challenges. The  
21 HMM framework contains a likelihood model which compares tag-recorded environmental  
22 data (depth, temperature, tidal characteristics) with those derived from an oceanographic  
23 model and a behavior model which constrains the horizontal movement of the fish. Validation  
24 experiments were performed on stationary tags, double-electronic-tagged fish (archival  
25 and acoustic tags), and simulated tracks. Known data, including fish locations and activity  
26 metrics, showed good agreement with those estimated by the modified approach, and  
27 improvements in performance of the modified method over the original. The modified ge-  
28 olocation approach will be applicable to additional species and regions to obtain valuable  
29 movement information that is not typically available for demersal fishes.

30

31 **Key words:** geolocation, hidden Markov model, fish migration, Atlantic cod,  
32 **Gadus morhua, data storage tags**

## 33 Introduction

34 The population structure of many fishery resources is more complex than the homogeneous  
35 units that are typically assumed in stock assessments and fishery management (Cadrin and  
36 Secor 2009). Recent research has increasingly focused on developing methods for incorpo-  
37 rating complex population structures. In order to incorporate these spatial processes into  
38 stock assessment models and fishery management plans, it is essential to have a proper un-  
39 derstanding of the movement of the species (Cadrin and Secor 2009; Goethel et al. 2011).  
40 The most common approach to studying movement of marine fish has been mark-recapture  
41 studies with conventional tags (Hall 2014). Conventional tags can provide information on  
42 general movements, but are not well suited for understanding behavioral patterns because  
43 they do not always reliably inform the trajectory of movement from release to recapture  
44 locations. In addition, conventional tagging typically relies on fishery-dependent recaptures,  
45 which can be biased by reporting rates and the distribution of fishing effort (Bolle et al.  
46 2005).

47 To address these limitations, geolocation methods have been developed to utilize elec-  
48 tronic tagging data to provide information about fish movements, distribution and behavior  
49 by estimating daily positions while fish are at liberty. Geolocation estimates are based on  
50 comparison of environmental data acquired from electronic tags (*e.g.*, temperature, pressure)  
51 with regional environmental databases (Evans and Arnold 2009). Geolocation methods have  
52 primarily utilized environmental data from recovered archival data storage tags (DSTs),  
53 including temperature, salinity, pressure (depth), and tidal data (amplitude/phase, tidal  
54 range/time of high water) (Arnold and Dewar 2001; Galuardi and Lam 2014), and these

55 methods have been applied to demersal groundfish. Alternative approaches based on light  
56 as well as satellite-based geolocation have been used for pelagic fishes and marine mammals  
57 ([Arnold and Dewar 2001](#); [Block et al. 2011](#); [Pedersen et al. 2011a](#)), but are not applicable  
58 to benthic species due to attenuation of these signals in the water column.

59 Prior work in the geolocation of demersal fish can be categorized into two fundamental  
60 approaches: algorithmic methods and State Space Models (SSMs). In the algorithmic class  
61 of schemes (*e.g.* [Hunter et al. 2003](#); [Gröger et al. 2007](#); [Neuenfeldt et al. 2007](#)), positions at  
62 each time step (*e.g.* daily) are determined using a direct comparison of the environmental  
63 data recorded by the DST with data derived from regional observations or an oceanographic  
64 model. Algorithmic approaches lack the intrinsic ability to quantify uncertainty, which is a  
65 significant drawback given the potential for location errors to arise from noisy observations  
66 and environmental data ([Patterson et al. 2008](#); [Thygesen et al. 2009](#)). In addition, a robust  
67 behavior model is often absent in algorithmic methods and conservative assumptions such  
68 as swimming speed constraints are instead applied. In contrast, state space models are  
69 statistical frameworks that can infer a series of state variables that are not directly measured,  
70 based on a series of observations that are conditioned on these unknown states. In the context  
71 of marine fish geolocation, the unknown states represent geographical locations of marine  
72 fish and the observation series is data recorded by DSTs ([Patterson et al. 2008](#); [Jonsen et al.](#)  
73 [2013](#)). Approaches based on state space models are largely able to overcome the drawbacks  
74 of algorithmic methods, because the uncertainty associated with the geolocations can be  
75 estimated, and a movement model describing the fish movement processes can be fit with  
76 observed data ([Jonsen et al. 2013](#); [Winship et al. 2012](#)).

77 An important geolocation methodology based on the state space model framework is the

78 hidden Markov model (HMM)(Pedersen et al. 2008, 2011a). The HMM is a form of state  
79 space model that deals with discrete states. In HMM, the estimation of the geographical  
80 location  $\mathbf{x}$  is explicitly represented by a probability density function  $\phi(\mathbf{x}, t)$ . In each time  
81 step, the observation is dependent on the corresponding hidden state. Such dependency  
82 can be described by a likelihood model, represented by probability density functions con-  
83 structed by comparing environmental data recorded by the tag with those from a model  
84 (*e.g.*, twilight light level model for light-based methods, oceanographic model for tidal- or  
85 depth/temperature-based methods). The hidden state sequence is a Markov chain bearing  
86 the assumption that the state at each time is dependent on the state at the previous time.  
87 Such dependency can be described by the behavior model. The output of an HMM is the es-  
88 timated hidden time series of geographical locations and the associated posterior probability  
89 distribution functions.

90 The HMM method has been applied to the geolocation of Atlantic cod (*Gadus morhua*)  
91 in multiple regions (*e.g.*, North Sea (Pedersen et al. 2008; Thygesen et al. 2009), Gulf of St.  
92 Lawrence (Le Bris et al. 2013a,b), Iceland (Thorsteinsson et al. 2012)), as well as European  
93 seabass (*Dicentrarchus labrax*) along the west coast of France (Wuillez et al. 2016). These  
94 efforts all used an open source MATLAB-based HMM geolocation toolbox developed by  
95 Pedersen (2008) (hereafter referred to as HGT), which is an implementation of a full HMM  
96 geolocation model. The kernel of HGT uses Bayes’ theorem to calculate the normalized  
97 conditional probability distribution  $\phi$  by performing a “time update” and an “observation  
98 update” during each timestep (Thygesen et al. 2009). Construction of  $\phi(\mathbf{x}, t)$  enables the  
99 calculation of the most probable track (MPT). All Bayesian calculations in HGT are con-  
100 ducted on a regular orthogonal grid in a geographic coordinate system with a fixed spatial

101 resolution.

102 A key challenge in the development of toolboxes such as HGT stems from the difficulty of  
103 generalizing the approach. For region- and species-specific applications of HMM geolocation,  
104 such models need careful calibration with available datasets. Environmental variables with  
105 the greatest spatial heterogeneity are most effective for geolocation. Therefore, the vari-  
106 ables that are most useful for geolocation frequently vary by region. For example, previous  
107 groundfish geolocation efforts utilized different environmental variables such as tidal data  
108 in the North Sea ([Metcalf and Arnold 1997](#); [Hunter et al. 2003, 2004](#); [Wright et al. 2006](#);  
109 [Thorsteinsson et al. 2012](#)), depth and salinity in the Baltic Sea ([Neuenfeldt et al. 2007](#)), and  
110 depth and temperature in Gulf of St. Lawrence ([Le Bris et al. 2013a,b](#)) to help distinguish  
111 between horizontal locations.

112 Assessing the quality of position estimates is a key component to the development of new  
113 geolocation techniques. Previous studies have assessed the accuracy of DST-based geoloca-  
114 tion using various approaches. One straightforward method is to compare the environmental  
115 parameters (*e.g.*, temperature, depth) measured by the tag with those estimated from the  
116 geolocated track ([Neuenfeldt et al. 2007](#)). However, a track whose corresponding environ-  
117 mental data matches the tag-measured values is not always biologically realistic ([Brickman  
118 and Thorsteinsson 2008](#)). Another approach to quantifying the accuracy of the track is  
119 to compare the estimated and true recapture location ([Hunter et al. 2003](#)). However, the  
120 premise of this method is the exclusion of the known recapture location from use in the  
121 geolocation process. Such exclusion may compromise the quality of the geolocation results,  
122 because the recapture location is a critical piece of information, especially for state space  
123 model-based methodologies with backward smoothing steps that propagate the recapture

124 location information back to the whole time series. Other previous validation methods in-  
125 clude geolocating DSTs moored on the bottom at fixed locations using tidal data ([Hunter](#)  
126 [et al. 2003](#); [Thorsteinsson et al. 2012](#)), double-tagging the free swimming fish with two dif-  
127 ferent type of electronic tags ([Teo et al. 2004](#); [Winship et al. 2012](#)), and generating known  
128 movement tracks of virtual fish using simulation ([Righton and Mills 2008](#)). None of these  
129 approaches has been applied to state space model-based geolocation methodologies using  
130 depth and temperature data recorded by DSTs.

131 In the present work, we focus on the geolocation of Atlantic cod tagged with DSTs off  
132 New England, USA. Atlantic cod are an economically-important groundfish species for New  
133 England fisheries and many prior conventional tagging studies have been conducted ([Hunt](#)  
134 [et al. 1999](#); [Howell et al. 2008](#); [Tallack 2011](#); [Loehrke 2013](#)). However, uncertainties remain  
135 with respect to cod behavior, movements, and stock structure, including the connectivity  
136 among subpopulations([Zemeckis et al. 2014b](#)). In order to utilize HGT for the geolocation,  
137 several modifications are necessary. Firstly, due to inadequate spatial contrast in tidal char-  
138 acteristics in the western Gulf of Maine, the full tidal-based likelihood model in HGT must  
139 be modified to use other environmental variables. Secondly, as identified by [Pedersen \(2007\)](#),  
140 the land treatment in the HGT behavior model simply masks out cells that represent land,  
141 which potentially allows a fish to cross land. This is especially problematic in our region of  
142 interest due to the presence Cape Cod, a narrow and elongated land feature (Fig. 1). Mod-  
143 ifications of the HMM methods in HGT were aimed at improving its performance for the  
144 current application, with consideration of also making it better suited for geolocating other  
145 groundfish species in the Gulf of Maine as well as other geographical areas. To achieve this  
146 objective, we made methodological contributions to the HMM geolocation package including

147 incorporation of a depth- and temperature-based likelihood model with tidal-based exclusion  
148 in the HMM framework, and employed quantitative error assessment of the geolocation re-  
149 sults using multiple approaches, including stationary mooring tags, double-electronic-tagged  
150 fish, and simulated tracks.

## 151 **Materials and Methods**

### 152 **Archival tagging**

153 As part of an interdisciplinary study, Atlantic cod were tagged with DSTs from 2010 through  
154 2012 in the Spring Cod Conservation Zone (SCCZ, Fig. 1) (Dean et al. 2014; Zemeckis et al.  
155 2014a; Zemeckis 2016), which is a seasonal spawning closure in northern Massachusetts Bay  
156 in the western Gulf of Maine (Armstrong et al. 2013). The DSTs deployed on a total of  
157 266 Atlantic cod were Star-ODDI milli-L tags (39.4 mm × 13 mm, depth range 1–250 m;  
158 Star-ODDI Ltd., Reykjavik, Iceland). From these studies, a total of 49 DSTs were recovered  
159 from recaptured fish with data suitable for geolocation. The resolution and accuracy of  
160 pressure (depth) measurements was 0.03% and  $\pm 0.8\%$  of the calibrated depth range (1-  
161 250 m), respectively. The resolution of temperature measurements was 0.032 °C and the  
162 accuracy was  $\pm 0.1$  °C. The DSTs were programmed to record pressure and temperature  
163 measurements every 15 min and 2 h 45 min, respectively. To be consistent with depth data,  
164 temperature data were later interpolated to 15 min intervals using cubic spline interpolation  
165 (Trauth et al. 2007). Locations of release and recapture of tagged fish were also recorded.  
166 Each recapture location was assigned an uncertainty level of low (15 km) or moderate (30

167 km) based on the type of fishing gear (i.e. fixed or mobile) used to capture the tagged fish  
168 and the reliability of the positions based on the reported format (GPS coordinates, LORAN  
169 coordinates, or descriptive locations with reference to landmarks). Uncertainty was greater  
170 (moderate) for fish caught in mobile trawl gear due to the average tow distance by trawlers  
171 targeting cod in the Gulf of Maine ( $15.8 \pm 9.3$  km) and for reported recaptures that were  
172 not in GPS format and therefore less precise.

173 To provide an independent set of location estimates of better accuracy as a means of val-  
174 idating geolocation results, the DST recaptures included ten fish that also had a surgically-  
175 implanted Vemco V16P-6H coded acoustic transmitter (Vemco Division, AMIRIX Systems,  
176 Inc., Nova Scotia, Canada) ([Zemeckis et al. 2014a](#)). These double-electronic-tagged cod were  
177 in spawning condition when released ([Dean et al. 2014](#)). Between 2010–2014, acoustic re-  
178 ceiver arrays were deployed to monitor cod spawning activity, including a Vemco Positioning  
179 System (VPS) in the cod conservation zone (see Fig. 2 in [Dean et al. 2014](#)) and acoustic  
180 receivers on both Eagle Ridge in Massachusetts Bay ( $\sim 15$  km south of the cod conservation  
181 zone) and Whaleback in Ipswich Bay ( $\sim 45$  km north of the cod conservation zone) ([Zemeckis](#)  
182 [2016](#)). The positioning system in the cod conservation zone covered  $9.5 \text{ km}^2$  and was able to  
183 determine horizontal positions with  $<10$  m of error ([Dean et al. 2014](#)). In addition, acoustic  
184 receivers were deployed in Massachusetts Bay and off Cape Ann to monitor the movements  
185 of striped bass (*Morone saxatilis*) with the maximum detection range estimated at  $\sim 1$  km  
186 (see Fig. 1 in [Kneebone et al. 2014](#)).

## 187 Oceanographic model environmental data

188 We used bottom water temperature and bathymetry data from the Northeast Coastal Ocean  
189 Forecasting System (Beardsley et al. 2013; NECOFS 2013), which is based on the unstruc-  
190 tured grid Finite-Volume Community Ocean Model (FVCOM) (Chen et al. 2006; Cowles  
191 et al. 2008). The NECOFS domain includes the entirety of the Gulf of Maine, Georges  
192 Bank, and the New England Shelf (Fig. 1), which covers all locations where cod from the  
193 western Gulf of Maine would be expected to be found based on observations from previous  
194 conventional tagging studies. The model mesh contains 90,415 elements in the horizontal  
195 grid and 45 vertical layers. The horizontal resolution ranges from 5 km near the open bound-  
196 ary to 500 m along the coast and tidal mixing fronts. The model is forced with hydrography  
197 and sea surface height at the open boundary, buoyancy flux from the major regional rivers,  
198 and wind stress and heat flux derived from regional hindcasts of the Weather Research and  
199 Forecasting (WRF) model. Observed data from moored arrays and sea surface tempera-  
200 ture are assimilated into the hindcasts. Model bathymetry is based on the regional USGS  
201 3-arcsec data product (Twomey and Signell 2013). NECOFS was hindcast for the period  
202 1978–present and hydrographic data, velocity, and sea surface height were archived at hourly  
203 intervals. For tidal information the eight primary regional constituents ( $M_2$ ,  $N_2$ ,  $S_2$ ,  $O_1$ ,  $K_1$ ,  
204  $K_2$ ,  $P_1$ , and  $Q_1$ ) were derived using harmonic analysis from a barotropic setup of NECOFS  
205 used to simulate regional tides. In comparison with data from 98 sea surface gauges, the  
206 standard deviation for the model-data difference of the  $M_2$  tidal constituent is 3.21 cm (Chen  
207 et al. 2011).

208 The NECOFS bottom water temperature is a critical component of the present geoloca-

209 tion effort. To assess the skill, model-computed bottom temperatures were compared with *in*  
 210 *situ* measurements collected during multiple field surveys carried out between 2003 and 2015  
 211 (Table 1). A total of 29,501 data points of measurements that are within the NECOFS model  
 212 domain cover the Gulf of Maine, Georges Bank, Southern New England and Mid Atlantic  
 213 Bight, and have not been assimilated to NECOFS. The overall mean of the model-observation  
 214 difference was  $-0.04\text{ }^{\circ}\text{C}$  and the overall RMSE was  $1.61\text{ }^{\circ}\text{C}$ . The model-observation discrep-  
 215 ancies did not exhibit significant seasonal or regional variation within the Gulf of Maine.  
 216 Based on data from NECOFS, a typical range of bottom temperature across the Gulf of  
 217 Maine and Georges Bank is approximately  $7\text{ }^{\circ}\text{C}$ , a variation which is large compared to  
 218 the NECOFS bottom temperature error. Following [Willmott \(1981\)](#), the NECOFS bottom  
 219 temperature data was also examined using the non-dimensional metric:

$$220 \quad W_s = 1 - \frac{\sum |T_{mo} - T_{me}|^2}{\sum (|T_{mo} - \overline{T_{me}}| + |T_{me} - \overline{T_{me}}|)^2}, \quad (1)$$

221 where  $T_{me}$  is the bottom temperature measurements,  $T_{mo}$  is the corresponding temperature  
 222 from NECOFS, and the overbar denotes a mean. As opposed to the more broadly considered  
 223  $R^2$ , the Willmott score is able to distinguish constant or proportional offset between the two  
 224 variables ([Willmott 1981](#)), and is commonly used in oceanographic model skill assessment  
 225 studies (*e.g.* [Warner et al. 2005](#); [Wilkin 2006](#); [O'Donncha et al. 2015](#)). The skill score  $W_s$   
 226 has a range of 0–1, with 1 indicating perfect agreement between model and measurement  
 227 and 0 indicating complete disagreement. For this comparison the skill value was 0.925,  
 228 demonstrating strong agreement. In conclusion, the NECOFS bottom temperature data is  
 229 generally appropriate for application to regional geolocation.

## 230 **Hidden Markov model design**

231 Geolocations for double-electronic-tagged cod were initially estimated using the original HGT  
232 which required only minor modification to work with NECOFS bathymetry and tidal data.  
233 These tracks were validated by comparison against acoustic telemetry data which provided  
234 known positions while the cod were at liberty (Supplementary Material). This study indi-  
235 cated that the accuracy of position estimates for the cod provided by the original HGT were  
236 not satisfactory for studying seasonal movement patterns of cod (median error >30 km),  
237 due primarily to inadequate spatial contrast in tidal characteristics, fish activity levels, and  
238 regional oceanographic conditions. We sought to improve HGT for application in the Gulf  
239 of Maine region, and provide a mechanism for enhanced performance in other regions and  
240 with other species. Building on previous work that aimed at assigning daily positions to  
241 statistical areas based upon DST data (Zemeckis 2016), revisions were made to the likeli-  
242 hood model, behavior model, and the most probable track construction in HGT. The HMM  
243 framework from the original HGT was maintained to calculate the posterior daily probability  
244 distribution of the fish. The source code of the modified HMM geolocation toolbox (revised  
245 HGT) is available at [https://github.com/cliu3/hmm\\_smast](https://github.com/cliu3/hmm_smast). The domain for all HMM  
246 calculations presented in this paper ranges from 71°W to 62°W and 40°N to 45°N, including  
247 most of the Gulf of Maine and Georges Bank at a resolution of 0.05° which is approximately  
248 equal to 4 km.

## 249 Likelihood model

250 Likelihood distributions were derived using a comparison of depth, water temperature, and  
251 tidal information extracted from DSTs with the corresponding estimates from the oceanographic  
252 model. Daily likelihood distributions  $L(\hat{\mathbf{x}})$ , representing the probability of the observation  
253 data given the discrete horizontal geographical location  $\hat{\mathbf{x}}$ , were constructed on the vertices  
254 of the unstructured grid of the oceanographic model. The approach considered the influence  
255 of temperature and depth separately from that of tides. Limited regional variation of the  
256 tidal characteristics in the western Gulf of Maine (Chen et al. 2011) reduces the utility  
257 of tides for geolocation. The  $M_2$  amplitude and phase may vary by only 0.25 m and  $15^\circ$ , respectively  
258 across a distance of 130 km. Additionally, off-bottom movement of fish can reduce or  
259 eliminate the ability to detect tide in the pressure signal. Considering these two factors,  
260 a geolocation method based solely on tidal information is not capable of producing sufficient  
261 accuracy in the Gulf of Maine for studying seasonal movement patterns of demersal fishes.  
262 Nonetheless, useful information may still be extracted from the tide signal. In the present  
263 work, an initial likelihood distribution  $L_{dt}(\hat{\mathbf{x}})$  was constructed using depth and temperature  
264 information. Tide, when available, was then used for eliminating unlikely regions in the final  
265  $L(\hat{\mathbf{x}})$  distribution.

266 The specific parameterization of the likelihood function depends on the daily activity of  
267 each fish, which was categorized as low, medium, or high using pressure data from the DST.  
268 We employed the tidal fitting procedure of Pedersen (2007), which calculates the least-square  
269 fit of the depth signal with a sinusoidal wave. Days were categorized as low activity when  
270 there was a satisfactory fit over a 13 h window, moderate activity days were identified as

271 those with satisfactory fits when using a 5 h window, and high activity days were those  
 272 during which there were no reliable tidal fits (Fig. 2). This classification is based on the  
 273 assumption that longer tidal fit represents demersal behavior at a fixed location and depth,  
 274 and therefore less horizontal movement. The criteria for goodness of fit for detection of tidal  
 275 signal was strict (root mean square error (RMSE)  $< 0.35$  m,  $R^2 > 0.92$ , and tidal amplitude  
 276 between 0.2 m and 2.0 m) to prevent false tidal fits which compromised estimates of tidal  
 277 phase and therefore geographic position. In contrast, a more relaxed tidal fitting criteria was  
 278 employed for identifying moderate activity periods ( $R^2 > 0.85$ ), because tidal characteristics  
 279 were not used for geolocation on moderate activity days.

280 Assuming that depth and temperature were independent, an initial likelihood distribution  
 281  $L_{dt}(\hat{\mathbf{x}})$  given the observed depth and temperature ( $z, T$ ) is obtained by forming the product  
 282 of two integrated normal distributions (modified from [Le Bris et al. 2013b](#)):

$$L_{dt}(\hat{\mathbf{x}}) = \int_{z-\Delta z}^{z+\Delta z} N(z; \mu_z(\hat{\mathbf{x}}), \sigma_z(\hat{\mathbf{x}})) dz \times \int_{T-\Delta T}^{T+\Delta T} N(T; \mu_T(\hat{\mathbf{x}}), \sigma_T(\hat{\mathbf{x}})) dT, \quad (2)$$

283 where  $\Delta z$  and  $\Delta T$  are the tag measurement error for depth and temperature, respectively,  
 284  $N(\mu, \sigma^2)$  is a normal distribution function of mean  $\mu$  and standard deviation  $\sigma$ , and  $\mu_z$  and  
 285  $\mu_T$  are NECOFS depth and temperature. The standard deviations of bathymetry  $\sigma_z(\hat{\mathbf{x}})$  and  
 286 temperature  $\sigma_T(\hat{\mathbf{x}})$  were determined using the NECOFS depth and temperature values from  
 287 the neighboring vertices of  $\hat{\mathbf{x}}$  on the unstructured grid. During low and moderate activity  
 288 periods,  $z$  and  $T$  were established using the mean depth and temperature over the satisfac-  
 289 tory tidal fit. Taking an average over the depth signal removes the sinusoidal tidal variation

290 and represents better the bathymetry of the fish's location, whereas the mean temperature  
 291 is an appropriate choice for comparison with the NECOFS daily-averaged bottom tempera-  
 292 ture data. During high activity periods, the depth-based likelihood factor is replaced by a  
 293 bathymetry uncertainty, after Pedersen (2007):

$$294 \quad L_{dt}(\hat{\mathbf{x}}) = \Phi\left(\frac{z - \mu_z(\hat{\mathbf{x}})}{\sigma_z(\hat{\mathbf{x}})}\right) / \Phi\left(\frac{-\mu_z(\hat{\mathbf{x}})}{\sigma_z(\hat{\mathbf{x}})}\right) \times \int_{T-\Delta T}^{T+\Delta T} N\left(T; \mu_T(\hat{\mathbf{x}}), \sigma_T(\hat{\mathbf{x}})\right) dT, \quad (3)$$

295 where  $\Phi$  is the cumulative density function of a standard Gaussian distribution,  $z$  and  $T$   
 296 were set using the depth and temperature when the fish was at its maximum depth during  
 297 the daily interval. This treatment is based on the constraint that the depth of the fish is  
 298 always less than the local bathymetry and accounts for bathymetry uncertainty.

299 When available, tidal information derived from tag data was used to eliminate unlikely  
 300 locations from the initial likelihood distribution. During low activity periods, the tag tidal  
 301 signal ( $\eta$ ) was compared with tidal signals for the same period from the oceanographic model  
 302 ( $\hat{\eta}(\hat{\mathbf{x}})$ ) using the root-mean-square deviation (RMSD) of the two time series at each NECOFS  
 303 grid point  $\hat{\mathbf{x}}$ :

$$304 \quad RMSD(\hat{\mathbf{x}}) = \sqrt{\frac{1}{n} \sum_{i=1}^n (\hat{\eta}_i(\hat{\mathbf{x}}) - \eta_i)^2}, \quad (4)$$

305 where  $n$  is the number of measurements in the 13-hour time series of the tide signal on a  
 306 given day. The initial likelihood distribution  $L_{dt}(\hat{\mathbf{x}})$  was then preserved at grid points where  
 307 two conditions were met: 1) the semi-diurnal amplitude of the tag signal  $A(\eta)$  is bounded by  
 308 the amplitude of  $M_2$  minus that of the sum of the other seven tidal constituents  $A_{M_2-\Sigma 7}(\hat{\mathbf{x}})$   
 309 and the sum of all eight principal tidal constituents  $A_{\Sigma 8}(\hat{\mathbf{x}})$ ; and 2) the RMSD was smaller

310 than a threshold value  $\Theta$  which was the 30th percentile of the RMSD calculated for the  
 311 remaining grid points. Implementation of the first condition avoids the computation effort  
 312 for reconstructing tidal signals ( $\hat{\eta}$ ) on grid points where the semi-diurnal amplitude clearly  
 313 do not match that of the tag signal. In the second condition, the value of  $\Theta$  was established  
 314 using performance testing which found that it was able to eliminate obviously spurious  
 315 position assignments. In addition, it also preserved  $L(\hat{\mathbf{x}})$  within a fairly broad horizontal  
 316 scale so that potential true positions do not get excluded. This scale was determined based  
 317 on the observed error of the double-electronic-tagged cod using the original HGT. For grid  
 318 points not meeting these two criteria, the likelihood was assigned a zero value (Fig. 3). In  
 319 summary, the final likelihood distribution  $L(\hat{\mathbf{x}})$  with tidal exclusion can be expressed as:

$$320 \qquad L(\hat{\mathbf{x}}) = L_{dt}(\hat{\mathbf{x}})H(\hat{\mathbf{x}}), \qquad (5)$$

321 where

$$322 \qquad H(\hat{\mathbf{x}}) = \begin{cases} 1, & \text{RMSD}(\hat{\mathbf{x}}) \leq \Theta \\ & \text{and } A(\hat{\eta}) \in [A_{M_2-7}(\hat{\mathbf{x}}), A_8(\hat{\mathbf{x}})] \\ 0, & \text{all other positions} \end{cases}. \qquad (6)$$

323 For days when tidal information was insufficient or absent from the tag data (i.e. during  
 324 moderate or high activity), tidal exclusion was not employed:

$$325 \qquad L(\hat{\mathbf{x}}) = L_{dt}(\hat{\mathbf{x}}). \qquad (7)$$

326 **Behavior model**

327 The behavior model describes the time evolution of the state variable, which is the daily  
328 movement of the fish. The horizontal movement of fish can be represented as a random walk  
329 (Sibert et al. 1999) which can be mathematically described using the Fokker-Planck diffusion  
330 equation:

$$331 \quad \frac{\partial \phi}{\partial t} = D \nabla^2 \phi, \quad (8)$$

332 where  $\phi$  is the probability density of the fish's location and  $D$  is a constant diffusivity  
333 coefficient, which is related to the swimming speed of the fish. The discretization scheme of  
334 the diffusion process was previously implemented in HGT following Thygesen et al. (2009),  
335 using a transition probability matrix representing an isotropic Gaussian kernel corresponding  
336 to the solution of Eq. 8. In this approach, the matrix is defined as  $\mathbf{H} = (\lambda_{ij})$ , where element  
337  $(i, j)$  represents a spatial location, and  $\lambda_{ij}$  represents the probability that the fish moves  
338 from the center element of  $\mathbf{H}$  to element  $(i, j)$ . The isotropic approach handles dry land  
339 by simply setting transition probabilities in these elements to zero (Thygesen et al. 2009;  
340 Pedersen et al. 2011a), allowing artificial crossing of fish from one side of a peninsula or other  
341 small scale land features to the other within a single time step. To prevent such infeasible  
342 results, the generation of the transition probability matrix was modified in the revised HGT.  
343 The transition probability matrix  $\mathbf{H}$  was first initialized as an empty matrix, with elements  
344 representing land masked out. A breadth-first searching algorithm was then used to generate  
345 a distance field  $\mathbf{S} = (s_{ij})$  of the same size as the transition probability matrix, with values  
346 equal to the shortest apparent distance from each element to the center element of the  
347 matrix around any masked-out obstacles. The values of the transition probability matrix  $\lambda_{ij}$

348 were then reassigned by evaluating the original Gaussian function at values of the apparent  
349 distance field  $\mathbf{S}$ . The effect of this treatment near land is equivalent to that of a reflecting  
350 boundary condition.

351 The behavior switching scheme described in Pedersen et al. (2008) which makes use of the  
352 activity level classification (Fig. 2) was also used in this work. A lower value of the diffusivity  
353 coefficient  $D$  was used for low and moderate activity days and a higher  $D$  for high activity  
354 days. The values of  $D$  can be specified as constant values or estimated using maximum  
355 likelihood estimation (MLE) (Pedersen et al. 2008). For simplicity and inclusiveness, in this  
356 study  $D$  was assigned constant values of  $10 \text{ km}^2/\text{d}$  as the lower value and  $100 \text{ km}^2/\text{d}$  as the  
357 higher value. This decision was based on the estimation of  $D$  from fish swimming speed  
358 presented by Pedersen (2007) considering the typical swimming speed of cod (Fernö et al.  
359 2011) and allowing for broader ranges of horizontal movement.

### 360 **Most probable track**

361 In the original HGT, the most probable track is one that maximizes the overall probability  
362 score of the whole sequence of locations using the Viterbi algorithm (Pedersen 2007; Thygesen  
363 et al. 2009), and the end point of the most probable track was set to be the grid cell where  
364 the value of the probability distribution  $\phi$  on recapture day is the greatest. We modified  
365 the approach to make sure the end point of the estimated MPT is close to the reported  
366 recapture location. The final point of the tag deployment was set to be the grid cell with  
367 the maximum  $\phi$  value among the cells that are within the uncertainty radius of the reported  
368 recapture location. This modification effectively nudges the estimated location on the day  
369 of recapture to be within the uncertainty radius of the reported recapture location.

370 In summary, the original HGT consists of a tidal-based likelihood model, a spatially dis-  
371 cretized Gaussian behavior model with simple land treatment, and an MPT search scheme  
372 based on the Viterbi algorithm. Modifications made in the revised HGT include the utiliza-  
373 tion of tag-recorded depth and temperature and the exclusion of unlikely locations based  
374 on tidal characteristics for the likelihood model, the activity classification based on length  
375 of tidal signal detection, improved land treatment in the behavior model, and a method  
376 to constrain the end point of the most probable track to be near the reported recapture  
377 location.

## 378 **Validation experiments**

379 To examine the performance of the revised HGT, the method was applied to two classes of  
380 DST datasets (including depth and temperature) with known locations. The first, bottom-  
381 mooring tags, challenge the model to maintain a fixed position over time. The second  
382 class of dataset consists of double-electronic-tagged fish that provide known locations that  
383 enable direct quantification of model skill when they pass through acoustic receiver arrays.  
384 This second class is useful for providing confidence in the geolocation, because the data is  
385 obtained from the tagged fish. To examine whether the revised HGT improves geolocation  
386 performance, the performance of the original HGT was also assessed using these two classes  
387 of DST datasets for comparison.

388 Another approach for validating the geolocation methodology is to assess the model's  
389 ability to replicate simulated tracks. Data for these fish were generated by interpolating  
390 pressure and temperature from the oceanographic model onto artificially constructed tracks.

391 In this study, simulated fish tracks were generated to examine the effect of season, region,  
392 and time at liberty on the accuracy of the geolocation results. The release positions were  
393 informed by the time and location of cod presence within the western Gulf of Maine inferred  
394 by recapture positions from conventional tag studies (Zemeckis 2016; Zemeckis et al. 2017).  
395 Movement tracks were simulated to occupy different regions (Gulf of Maine and Georges  
396 Bank) during two seasons (summer and winter) across a range of days at liberty (40 d, 120  
397 d, and 360 d)(Fig. 4). Daily locations for each track were generated using a random walk  
398 with the following equation:

$$399 \quad \mathbf{X}_{t+1} = \mathbf{X}_t + R\sqrt{2D\delta t}, \quad (9)$$

400 where  $\mathbf{X}_{t+1}$  and  $\mathbf{X}_t$  are locations in the simulated track on day  $t+1$  and  $t$ , respectively,  $R$  is  
401 a random factor producing a standard normal distribution (zero mean and unit variance),  $D$   
402 is the diffusivity having a value of 10 km<sup>2</sup>/d or 100 km<sup>2</sup>/d, and  $\delta t = 1$  d is the time interval.  
403 Simulated individuals were constrained to remain in the model domain. If an individual  
404 moved across land or open-ocean boundary during a time step  $t+1$ , it was restored to  
405 its last position (from the previous time step  $\mathbf{X}_t$ ). This boundary treatment method was  
406 chosen because of the ease of implementation within the unstructured mesh framework of  
407 NECOFS FVCOM. After the simulated track was generated, the corresponding depth and  
408 temperature time series were constructed at 15 min intervals using the tidal and bottom  
409 temperature data derived from the oceanographic model in order to create a simulated tag.  
410 No noise was added to the simulated depth and temperature signals. Ten simulation sets  
411 consisting of five runs each were performed. Each set was based on a unique combination  
412 of season, region, and time at liberty (Table 2). When performing geolocation using the

413 simulated data, release locations were used without uncertainty, while recapture location  
414 uncertainty was 15 km.

## 415 **Results**

### 416 **Geolocation Model Validation**

417 To validate the activity characterization approach of the likelihood model, we compared the  
418 size of the daily 95% utilization distribution derived from VPS detection reported in (Dean  
419 et al. 2014) with the daily activity levels determined by the likelihood model. The median  
420 areas of the daily 95% utilization distribution were 0.038 km<sup>2</sup> for the low activity days, 0.11  
421 km<sup>2</sup> for the moderate activity days, and 0.26 km<sup>2</sup> for the high activity days (Fig. 5). The  
422 relation between these two metrics shows a trend in which days classified as lower levels  
423 of activity based on vertical movements are those during which the fish utilized less space  
424 horizontally.

425 A total of 14 Star-ODDI DSTs were moored to different fixed locations on cod spawning  
426 sites in Massachusetts Bay and Ipswich Bay between 2010–2012 and Jeffreys Ledge between  
427 2014–2015 in order to test the performance of the DSTs and validate the geolocation method-  
428 ology. Geolocation using the revised HGT were performed on tag-recorded data from these  
429 deployments, in which release and recapture locations were used without uncertainty. Daily  
430 location estimations in the most probable track were compared with the known mooring  
431 locations. The most probable track estimations for the 14 mooring DST deployments were  
432 close to their deployment locations. The RMSE of the daily location estimation from all

433 mooring tags was 11.07 km and the error range was 0.14–25.51 km (Table 3a). The median  
434 geolocation error for all mooring tags was 4.93 km. This represents a significant improvement  
435 over the error of 33.94 km found using the original HGT (Table 3a, 3b). Tag #73 was the  
436 best performing deployment (Fig. 6a) with a median daily location error of 1.86 km, whereas  
437 tag no. 71 (off Provincetown, Cape Cod) was the worst performing deployment (Fig. 6c) with  
438 a median daily location error of 23.10 km. Tag no. 87, for which the median error was 4.79  
439 km, was representative of the overall mooring tag deployments (median 4.93 km) (Fig. 6b).  
440 To assess the accuracy of the constructed probability density functions, mean normalized  
441 probability at known locations were calculated for each track to give a value between 0 and  
442 1, where 1 indicates that the probability density function most accurately estimates the  
443 known locations, and 0 indicates that the probability density function is unable to correctly  
444 estimate the known locations. The overall mean normalized probability at known locations  
445 for all mooring tags ranged from 0.30 – 1, with an average of 0.69. Compared with the  
446 same metric derived from the original HGT (0.06), this represents a significant improvement  
447 (Table 3a, 3b).

448 High resolution positions of the double-electronic-tagged cod determined by acoustic  
449 receivers were compared to the same-day position estimates from the most probable track  
450 constructed by the revised HGT. To assess whether the revision to HGT improved geolocation  
451 results, acoustically detected location were also compared with position estimates using the  
452 original HGT with minimum changes only to enable the input of NECOFS bathymetry and  
453 tidal data. Most (217 out of 223, 97.3%) of the daily locations of the most probable track  
454 estimated by the revised HGT were within 42 km of the acoustically-detected locations  
455 (Fig. 7). The median geolocation error for the revised HGT was 6.45 km, which is an

456 improvement over the value of 34.80 km found using the original HGT (Table 3c, 3d,  
457 Supplementary Material Table S1). This reduction in error is essential for studying seasonal  
458 movement of cod in the Gulf of Maine, because all the double-electronic-tagged fish were  
459 recaptured within 82 km of their release location. The average normalized probability at the  
460 acoustically-detected locations was 0.47 for the revised HGT, much higher than that of the  
461 original HGT, 0.06 (Table 3c, 3d). Although the median geolocation error was less in the  
462 modified model, in rare cases (6 out of 223 estimates, <3%) errors in such estimates were  
463 found to be between 33–62 km greater than that of the original HGT. These six estimates  
464 also had the greatest error and were all from fish no. 22 which had the longest duration (212  
465 d) (Table 4).

466 In the simulated track experiments, the most probable track output was compared with  
467 the simulated tracks. The mean and median location estimation error for the simulated  
468 tracks were 92.40 km and 69.46 km, respectively. The mean normalized probability at  
469 known locations was 0.39. A breakdown of the daily location errors for all simulated tracks  
470 indicated variation of location errors among seasons, geographical regions, and numbers of  
471 days between release and recapture (Fig. 8). Across all seasons, the median error increased  
472 when fish were at liberty for a longer period. This finding is consistent with results from  
473 the double-electronic-tagging experiments which found that geolocation errors for cod were  
474 greater for cod that spent longer time in the water. For simulated runs with duration of 40  
475 d and 120 d, the median error during winter was greater than during summer. Estimated  
476 location errors of the Gulf of Maine tracks were slightly greater than those of the Georges  
477 Bank tracks in general, with the 120 d tracks released in winter as exceptions.

## 478 **Geolocation of the double-electronic-tagged cod**

479 The revised HGT was applied to the double-electronic-tagged fish ( $n=10$ ). All ten cod  
480 were recaptured in the Gulf of Maine and within 82 km of their release position in the cod  
481 conservation zone (Table 4, Fig. 9), with the average number of days at large being 79.5  
482 days. The distance between the reported and estimated recapture locations were all within  
483 the uncertainty radius around the reported recapture locations except fish no. 22, which  
484 exceeded its uncertainty radius of 30 km by 4.3 km. Five fish (nos. 7, 8, 11, 12, and 13) moved  
485 east towards Stellwagen Bank, with two (nos. 12 and 13) exhibiting a stationary period in  
486 southern Massachusetts Bay classified as mostly low activity days (Fig. 10). Geolocation  
487 results demonstrated that cod moved offshore after spawning. Most cod remained within  
488 the western Gulf of Maine. However, two fish (nos. 18 and 22) moved to the southeast towards  
489 the Great South Channel and Georges Bank before migrating north and being recaptured  
490 in the Gulf of Maine. These movements represent migrations across the current boundary  
491 between the Gulf of Maine and Georges Bank management units (see [NEFSC 2013](#)).

492 Cod no. 16 generally stayed in the cod conservation zone throughout its 27 days at liberty,  
493 corroborated by acoustic receiver detections being received on each day when it was at large  
494 with the exception of 21 June 2010. No. 17 traveled north towards Ipswich Bay, which is a  
495 major cod spawning ground during the spring. No. 24 moved to Stellwagen Bank and was  
496 later recaptured on southern Jeffreys Ledge.

## 497 Discussion

### 498 Geolocation methods

499 The geolocation method presented in this paper is a direct development from the HMM  
500 geolocation method presented by [Pedersen et al. \(2008\)](#) and implemented in HGT. New  
501 elements developed in the present geolocation method and implemented into the revised  
502 HGT have improved model performance for our application. These include the exclusion of  
503 unlikely locations based on tidal characteristics, the utilization of depth and temperature and  
504 the tidal-based activity classification for the likelihood model, improved land treatment in  
505 the behavior model, and a method to constrain the end point of the most probable track to be  
506 near the reported recapture location. The introduction of the moderate activity enhances the  
507 utility of vertical behavioral information. Validation in activity classification using the VPS  
508 occupancy utilization data links the horizontal and vertical movement of the fish. Although  
509 [Hobson et al. \(2009\)](#) concludes that there is no decisive connection from vertical behavior  
510 pattern of cod to its horizontal migration or residence behavior, our validation results indicate  
511 a pattern that cod tend to utilize larger areas when greater vertical activity is observed, which  
512 justifies the use of multiple values of the diffusivity coefficient  $D$  corresponding to different  
513 activity levels in the behavior model. One caveat of this validation is that such justification is  
514 based on data collected from a specific behavior period because the double-electronic-tagged  
515 cod were all in spawning condition, which may be a period when cod are more sedentary than  
516 they are at other times of the year. Also worth noting is that our behavior classifications are  
517 based on available behavioral observations and relevant to Gulf of Maine cod, whereas cod  
518 in other regions may exhibit different behavior. Secondly, the exclusion of unlikely locations

519 based on tidal characteristics was inspired by fully tidal-based methods (*e.g.* [Hunter et al.](#)  
520 [2003, 2004](#); [Gröger et al. 2007](#); [Pedersen et al. 2008](#)), which do not perform well in regions  
521 where tidal variation is small. Exploratory experiments in which tidal characteristics were  
522 incorporated in the joint likelihood distribution in a similar way with depth and temperature  
523 indicated that such inclusion misleads the location estimates in the western Gulf of Maine.  
524 By excluding unlikely locations, the accuracy of the likelihood model and the computational  
525 efficiency were improved. Therefore, this tidal exclusion scheme is the primary reason that  
526 the revised HGT demonstrated better performance over the original HGT in the mooring  
527 and double-tagging validation experiments. In the original HGT, the land treatment in the  
528 behavior model allowed unrealistic crossing of peninsulas and other promontories. [Pedersen](#)  
529 [et al. \(2011b\)](#) employed a finite element method to solve the nonlinear Bayesian fish tracking  
530 problem on domains with irregular geometry, which is an ideal method for land avoidance  
531 in terms of accuracy, but at the expense of computational efficiency. In our modification  
532 to the HGT we focused on using an approach that was straightforward to implement to  
533 improve the land treatment scheme without significantly increasing the computational load.  
534 Our modification eliminates the possibility of fish crossing over land. Lastly, confining the  
535 estimated recapture location of the most probable track near the reported recapture location  
536 resulted in a track that is more realistic.

## 537 **Accuracy of geolocation estimations**

538 This validation study is a comprehensive effort for DST-based geolocation methods applied  
539 to demersal fishes. Model validation experiments using fixed mooring tags and double-

540 electronic-tagged cod indicated that the revised HGT produces more accurate results than  
541 previous tidal- or light-based methods using archival tags. The estimated error using revised  
542 HGT for mooring tags at fixed locations was between 0.14 and 25.51 km, with a mean  
543 value of 11.07 km (Table 3a, Supplementary Material Table S1). [Hunter et al. \(2003\)](#) and  
544 [Thorsteinsson et al. \(2012\)](#) used mooring tags fixed at known locations to validate their  
545 tidal-based method and their reported average error was  $15.7 \pm 3.5$  km and 18.91 km,  
546 respectively. The root mean square error (RMSE) of our method for double-electronic-  
547 tagged fish was 21.87 km (Table 3b). Double-tagging studies of sharks ([Teo et al. 2004](#);  
548 [Winship et al. 2012](#)) found errors  $> 0.5^\circ$  (approximately equal to 55 km), but the error is  
549 likely greater for sharks since they tend to have higher horizontal speeds and travel more  
550 frequently than groundfish. [Righton and Mills \(2008\)](#) reported that the average error for  
551 their DST-based method using five 50-d simulated tracks determined by the most likely path  
552 using a highest total score approach was between 37 and 69 km. The median error of our  
553 40-d simulated track runs, which was determined by the most probable track using similar  
554 criteria maximizing the overall score, was 29.16 km.

555 Comparison of the geolocation results of the ten double-electronic-tagged cod using re-  
556 vised HGT with the statistical area assignment for the same cod (based on the common  
557 numbering listed in the “DMF Fish ID” column in Table 4) presented in [Zemeckis \(2016\)](#)  
558 and [Zemeckis et al. \(2017\)](#) indicated that the revised HGT was capable of providing superior  
559 geolocation estimates compared to a coarse scale algorithmic geolocation method. Although  
560 the two methods share the same likelihood model, by introducing HMM in the geolocation  
561 method, drawbacks in the previous algorithmic method that lead to occasionally erroneous  
562 position assignments were overcome in the revised HGT.

563 Geolocation of stationary tags indicated that the current method is able to provide highly  
564 accurate location estimates for fixed-location objects. Errors in archival tag measurements  
565 and depth and temperature data derived from the oceanographic model are potential sources  
566 of error in geolocation estimates of the fixed-location tags. In comparison, location estimation  
567 error was nearly doubled for the double-tagging experiment of free-swimming cod (Table 3).  
568 Such comparison indicates that the current behavior model may be another significant source  
569 of location error in addition to that induced by tag data and the oceanographic model  
570 errors; the current behavior model is likely the barrier to achieving highly accurate location  
571 estimates for free-swimming fish. A behavior model that more accurately describes the  
572 spatial movements of the fish species in question is expected to improve the accuracy of  
573 geolocation estimates. We assumed fish movement could be modeled with a random walk.  
574 The use of alternative schemes such as Brownian motion or Lévy flight have been shown to  
575 have a negligible effect on geolocation when compared with the random walk (Thygesen and  
576 Nielsen 2009). Moreover, the underlying behavior state time series of a fish can be estimated  
577 more accurately using a separate or extended state space model framework (Patterson et al.  
578 2009, 2016). Pedersen et al. (2011a) present a similar HMM framework which estimates  
579 behavior and movement at the same time. (Pedersen et al. 2011a) also includes a model  
580 selection scheme for the behavior model with a candidate set of models with different set of  
581 parameters including advection, which is not considered in the current method. However, the  
582 implementation of such behavior state schemes will increase the mathematical complexity  
583 and the computational intensity of the geolocation model. When considering alternative  
584 behavior models in future efforts, both the computational efficiency and the accuracy of the  
585 geolocation should be considered.

586 Geolocation results of stationary tags (Fig. 6) also suggest that spatially-varying sys-  
587 tematic biases may exist in geolocation estimates. Such biases may be caused by local  
588 bathymetry and oceanographic conditions that result in similar temperature and depth over  
589 a broader area. Similar phenomenon was reported for other telemetry techniques for estimat-  
590 ing fish locations and can be potentially corrected by deploying stationary tags throughout  
591 the study area ([Charles et al. 2016](#)). To better understand the effect of systematic biases  
592 in geolocation estimates, fixed-location mooring deployments are recommended for future  
593 geolocation tagging projects.

594 Simulated track experiment results suggested that geolocation estimates using revised  
595 HGT were more accurate for fish at liberty for fewer days, tagged during summer when  
596 spatial variation of bottom temperature is relatively large, and released in regions where  
597 bathymetric variation is large. The seasonality of geolocation accuracy was similar to the  
598 conclusions made by [Righton and Mills \(2008\)](#). These findings may provide guidance for  
599 future geolocation tagging to help achieve more accurate location estimates.

600 Exploratory analyses showed that geolocation estimates of the simulated tracks are more  
601 accurate using the original HGT compared with those of the present work. This finding  
602 is intuitive given the inherent differences between the two approaches. In these simulated  
603 tracks, the tidal signal is derived directly from the NECOFS database and thus the tidal  
604 model is effectively without error. In contrast to the revised HGT which employs the tidal  
605 signal for the purpose of exclusion, the original HGT incorporates the spatial variation  
606 of the tidal signal in the geolocation process and thus is able to take advantage of the  
607 perfect fit between the model and tag data in the simulations. With real tag data and an  
608 imperfect tidal database, attempts to incorporate directly the tidal information can have an

609 adverse effect on the geolocation accuracy ([Le Bris et al. 2013b](#)), as demonstrated in the  
610 aforementioned double-electronic-tagged experiments. Nonetheless, the original HGT may  
611 show good performance in areas where the variation in the spatial tidal characteristics is  
612 significant compared to errors associated with tag measurement and tidal database, such as  
613 the North Sea.

## 614 **Applications**

615 Results of this work may have implications for the regional fishery management of cod. The  
616 residency exhibited in geolocation estimates of eight double-electronic-tagged cod (nos. 7, 8,  
617 11, 12, 13, 16, 17, and 24) is similar to findings from previous conventional tagging studies  
618 ([Hunt et al. 1999](#); [Tallack 2011](#); [Loehrke 2013](#)) which classified cod in the Gulf of Maine as  
619 sedentary ([Howell et al. 2008](#)). However, such agreement may be a result of limited DST  
620 durations (<3 months) and limitations of conventional tagging comparing only release and  
621 recapture locations, both limitations tend to underestimate the horizontal activity of cod.  
622 Moreover, geolocation estimates of the other two double-electronic-tagged cod (nos. 18 and  
623 22) indicate movements across the current management unit boundary between the Gulf of  
624 Maine and Georges Bank management units, similar to the results of [Gröger et al. \(2007\)](#).  
625 Such movements would not have been observed with conventional tagging methods because  
626 these cod were released and recaptured in the same management unit. Results from further  
627 application of the geolocation method to available DST tag data of cod off New England  
628 may have important implications for future stock identification regarding the delineation of  
629 management unit boundaries.

630 The HMM-based geolocation method presented in this work is expected to be applicable  
631 to other demersal groundfish species. For example, within the northeast U.S. region alone,  
632 DSTs have been used to study multiple demersal species (*e.g.*, yellowtail flounder, [Cadrin  
633 and Westwood 2004](#); monkfish, [Grabowski et al. 2013](#); summer flounder, [Henderson and  
634 Fabrizio 2014](#); winter flounder, [Coleman 2015](#); black sea bass, [Moser and Shepherd 2009](#);  
635 Atlantic halibut, [Kanwit et al. 2008](#)). The lack of access to validated geolocation methods  
636 creates barriers to the process of deriving reliable movement information from the tag data.  
637 The current study provides a geolocation method that would be applicable to these other  
638 datasets, thereby breaking some of these barriers.

639 Global or regional oceanographic data that are relevant to the current HMM geolocation  
640 method, such as temperature, tides, and bathymetry, are readily available, which enables  
641 the applicability of the current HMM geolocation method to other regions. The Oregon  
642 State University Tidal Inversion Software (OTIS) and the associated MATLAB Tidal Model  
643 Driver toolbox ([Egbert and Erofeeva 2002](#)) are capable of providing global tidal harmonics  
644 data. Databases of ocean general circulation model (OGCM) output typically contain 4-  
645 dimensional sea water temperature. A review of some regional and global data products,  
646 including model descriptions and how to obtain model outputs, was given by [Potemra \(2012\)](#).  
647 For better accuracy of the geolocation estimates, the spatial resolution of such environmental  
648 data needs to be higher than the estimated location error scale.

649 We implemented an HMM-based geolocation model for Atlantic cod in the Gulf of Maine.  
650 The model framework utilizes temperature and depth data from DSTs for location estima-  
651 tion, and tidal data for exclusion of unlikely locations. A tidal-based daily activity level  
652 classification scheme was implemented to improve the accuracy of the likelihood distribution

653 and determine the behavior states. Comprehensive validation experiments were performed  
654 on stationary mooring tags, double-electronic-tagged fish, and simulated tracks. Validation  
655 results suggest good performance of the revised geolocation model and improvements in  
656 performance over the original approach. This method could be applied to other demersal  
657 groundfish species, and is relevant to future stock identification and fishery management.

## 658 **Acknowledgements**

659 The authors would like to thank the three reviewers for their valuable comments and sug-  
660 gestions that did much to improve the manuscript. Cod tagging research in the Spring Cod  
661 Conservation Zones was supported by the United States Fish and Wildlife Service through  
662 the Sportfish Restoration Act and the Massachusetts Marine Fisheries Institute. Funding  
663 for the research conducted as part of this manuscript was provided by NOAA Saltonstall-  
664 Kennedy Grant award NA15NMF4270267 and the University of Massachusetts Intercampus  
665 Marine Science (IMS) Graduate Program. Part of the HMM geolocation computations were  
666 made on the University of Massachusetts Dartmouth's GPGPU high performance computing  
667 cluster, which was acquired with support from NSF award CNS-0959382. The authors would  
668 like to thank William Hoffman, Michael P. Armstrong, and David Martins for assisting with  
669 fish tagging and data collection, Gregory DeCelles and N. David Bethoney for providing sur-  
670 vey data with bottom temperature measurements, Arnault Le Bris for providing feedback  
671 that has improved the manuscript, and Martin W. Pedersen for granting permission to reuse  
672 the HMM Geolocation Toolbox and providing technical advice.

## 673 **References**

- 674 Armstrong, M.P., Dean, M.J., Hoffman, W.S., Zemeckis, D.R., Nies, T.A., Pierce, D.E.,  
675 Diodati, P.J., and McKiernan, D.J. 2013. The application of small scale fishery closures  
676 to protect Atlantic cod spawning aggregations in the inshore Gulf of Maine. *Fish. Res.*  
677 **141**: 62–69. doi:10.1016/j.fishres.2012.09.009.
- 678 Arnold, G. and Dewar, H. 2001. Electronic tags in marine fisheries research: A 30-year  
679 perspective. In *Electronic Tagging and Tracking in Marine Fisheries*, edited by J.R. Sibert  
680 and J.L. Nielsen, Springer Netherlands, number 1 in *Reviews: Methods and Technologies*  
681 in *Fish Biology and Fisheries*, pp. 7–64. Doi: 10.1007/978-94-017-1402-0.2.
- 682 Beardsley, R.C., Chen, C., and Xu, Q. 2013. Coastal flooding in Scituate (MA): A FVCOM  
683 study of the 27 December 2010 nor'easter. *J. Geophys. Res.-Oceans* **118**(11): 6030–6045.  
684 doi:10.1002/2013JC008862.
- 685 Block, B.A., Jonsen, I.D., Jorgensen, S.J., Winship, A.J., Shaffer, S.A., Bograd, S.J., Hazen,  
686 E.L., Foley, D.G., Breed, G.A., Harrison, A.L., Ganong, J.E., Swithenbank, A., Castleton,  
687 M., Dewar, H., Mate, B.R., Shillinger, G.L., Schaefer, K.M., Benson, S.R., Weise, M.J.,  
688 Henry, R.W., and Costa, D.P. 2011. Tracking apex marine predator movements in a  
689 dynamic ocean. *Nature* **475**(7354): 86–90. doi:10.1038/nature10082.
- 690 Bolle, L.J., Hunter, E., Rijnsdorp, A.D., Pastoors, M.A., Metcalfe, J.D., and Reynolds, J.D.  
691 2005. Do tagging experiments tell the truth? Using electronic tags to evaluate conventional  
692 tagging data. *ICES J. Mar. Sci.* **62**(2): 236–246. doi:10.1016/j.icesjms.2004.11.010.

693 Brickman, D. and Thorsteinsson, V. 2008. Geolocation of Icelandic cod from DST data using  
694 a modified particle filter method. ICES CM 2008/P.09 .

695 Cadrin, S.X. and Secor, D.H. 2009. Accounting for spatial population structure in stock  
696 assessment: Past, present, and future. In *The Future of Fisheries Science in North America*,  
697 edited by R.J. Beamish and B.J. Rothschild, Springer Netherlands, number 31 in Fish &  
698 Fisheries Series, pp. 405–426. Doi: 10.1007/978-1-4020-9210-7\_22.

699 Cadrin, S.X. and Westwood, A.D. 2004. The use of electronic tags to study fish movement:  
700 a case study with yellowtail flounder off New England. ICES CM 2004/K **81**.

701 Charles, C., Gillis, D.M., Hrenchuk, L.E., and Blanchfield, P.J. 2016. A method of spatial  
702 correction for acoustic positioning biotelemetry. *Animal Biotelemetry* **4**: 5. doi:10.1186/  
703 s40317-016-0098-3.

704 Chen, C., Beardsley, R.C., and Cowles, G. 2006. An unstructured grid, finite-volume coastal  
705 ocean model (FVCOM) system. *Oceanography* **19**(1): 78.

706 Chen, C., Huang, H., Beardsley, R.C., Xu, Q., Limeburner, R., Cowles, G.W., Sun, Y., Qi,  
707 J., and Lin, H. 2011. Tidal dynamics in the Gulf of Maine and New England Shelf: An  
708 application of FVCOM. *J. Geophys. Res.-Oceans* **116**(C12). doi:10.1029/2011JC007054.

709 Coleman, K.E. 2015. Understanding the winter flounder (*Pseudopleuronectes americanus*)  
710 southern New England/Mid-Atlantic stock through historical trawl surveys and monitor-  
711 ing cross continental shelf movement. MS thesis, Rutgers University, New Brunswick,  
712 NJ.

- 713 Cowles, G.W., Lentz, S.J., Chen, C., Xu, Q., and Beardsley, R.C. 2008. Comparison of  
714 observed and model-computed low frequency circulation and hydrography on the New  
715 England Shelf. *J. Geophys. Res.-Oceans* **113**(C9): C09015. doi:10.1029/2007JC004394.
- 716 Dean, M.J., Hoffman, W.S., Zemeckis, D.R., and Armstrong, M.P. 2014. Fine-scale diel  
717 and gender-based patterns in behaviour of Atlantic cod (*Gadus morhua*) on a spawning  
718 ground in the Western Gulf of Maine. *ICES J. Mar. Sci.* **71**(6): 1474–1489. doi:10.1093/  
719 icesjms/fsu040.
- 720 Egbert, G.D. and Erofeeva, S.Y. 2002. Efficient inverse modeling of barotropic ocean  
721 tides. *J. Atmos. Oceanic Technol.* **19**(2): 183–204. doi:10.1175/1520-0426(2002)019<0183:  
722 EIMOBO>2.0.CO;2.
- 723 Evans, K. and Arnold, G. 2009. Summary report of a workshop on geolocation methods for  
724 marine animals. In *Tagging and tracking of marine animals with electronic devices*, edited  
725 by J.L. Nielsen, H. Arrizabalaga, N. Fragoso, A. Hobday, M. Lutcavage, and J. Sibert,  
726 Springer Netherlands, number 9 in *Reviews: Methods and Technologies in Fish Biology*  
727 and *Fisheries*, pp. 343–363.
- 728 Fernö, A., Jørgensen, T., Løkkeborg, S., and Winger, P.D. 2011. Variable swimming speeds  
729 in individual Atlantic cod (*Gadus morhua* L.) determined by high-resolution acoustic  
730 tracking. *Mar. Biol. Res.* **7**(3): 310–313. doi:10.1080/17451000.2010.492223.
- 731 Galuardi, B. and Lam, C.H.T. 2014. Telemetry analysis of highly migratory species. In  
732 *Stock Identification Methods (Second Edition)*, edited by S.X. Cadrin, L.A. Kerr, and  
733 S. Mariani, Academic Press, San Diego, pp. 447–476.

- 734 Goethel, D.R., Quinn, T.J., and Cadrin, S.X. 2011. Incorporating spatial structure in stock  
735 assessment: movement modeling in marine fish population dynamics. *Rev. Fish. Sci.*  
736 **19**(2): 119–136. doi:10.1080/10641262.2011.557451.
- 737 Grabowski, J., Sherwood, G.D., and Bank, C. 2013. Northeast regional monkfish tagging  
738 program: Additional archival tagging and otolith analyses to assess monkfish movements  
739 and age. Technical report. Final Report to the 2010 Monkfish Research Set Aside Program.
- 740 Gröger, J.P., Rountree, R.A., Thygesen, U.H., Jones, D., Martins, D., Xu, Q., and  
741 Rothschild, B.J. 2007. Geolocation of Atlantic cod (*Gadus morhua*) movements in  
742 the Gulf of Maine using tidal information. *Fish. Oceanogr.* **16**(4): 317–335. doi:  
743 10.1111/j.1365-2419.2007.00433.x.
- 744 Hall, D.A. 2014. Conventional and radio frequency identification (RFID) tags. In *Stock*  
745 *Identification Methods* (Second Edition), edited by S.X. Cadrin, L.A. Kerr, and S. Mariani,  
746 Academic Press, San Diego, pp. 365–395.
- 747 Henderson, M.J. and Fabrizio, M.C. 2014. Small-scale vertical movements of summer flounder  
748 relative to diurnal, tidal, and temperature changes. *Mar. Coast. Fish.* **6**(1): 108–118. doi:  
749 10.1080/19425120.2014.893468.
- 750 Hobson, V., Righton, D., Metcalfe, J., and Hays, G. 2009. Link between vertical and  
751 horizontal movement patterns of cod in the North Sea. *Aquat. Biol.* **5**: 133–142. doi:  
752 10.3354/ab00144.
- 753 Howell, W.H., Morin, M., Rennels, N., and Goethel, D. 2008. Residency of adult Atlantic

754 cod (*Gadus morhua*) in the western Gulf of Maine. Fish. Res. **91**(23): 123–132. doi:  
755 10.1016/j.fishres.2007.11.021.

756 Hunt, J.J., Stobo, W.T., and Almeida, F. 1999. Movement of Atlantic cod, *Gadus morhua*,  
757 tagged in the Gulf of Maine area. Fish. Bull. **97**(4): 842–860.

758 Hunter, E., Aldridge, J.N., Metcalfe, J.D., and Arnold, G.P. 2003. Geolocation of free-  
759 ranging fish on the European continental shelf as determined from environmental variables  
760 - I. Tidal location method. Mar. Biol. **142**(3): 601–609. doi:10.1007/s00227-0984-5.

761 Hunter, E., Metcalfe, J.D., Holford, B.H., and Arnold, G.P. 2004. Geolocation of free-  
762 ranging fish on the European continental shelf as determined from environmental variables  
763 - II. Reconstruction of plaice ground tracks. Mar. Biol. **144**(4): 787–798. doi:10.1007/  
764 s00227-003-1242-1.

765 Jonsen, I., Basson, M., Bestley, S., Bravington, M., Patterson, T., Pedersen, M., Thomson,  
766 R., Thygesen, U., and Wotherspoon, S. 2013. State-space models for bio-loggers: A  
767 methodological road map. Deep Sea Res. Part II **88-89**: 34–46. doi:10.1016/j.dsr2.2012.  
768 07.008.

769 Kanwit, K., De Graaf, T., and Bartlett, C. 2008. Biological sampling, behavior and migration  
770 study of Atlantic halibut (*hippoglossus hippoglossus*) and cusk (*brosme brosme*) in the Gulf  
771 of Maine, year 2. Final report submitted to the Northeast Cooperative Research Partners  
772 Program, Maine Department of Marine Resources. Available at [https://www1.maine.  
773 gov/dmr/science-research/species/documents/08halibutcusk.pdf](https://www1.maine.gov/dmr/science-research/species/documents/08halibutcusk.pdf). Accessed: 2016-  
774 8-12.

- 775 Kneebone, J., Hoffman, W.S., Dean, M.J., and Armstrong, M.P. 2014. Movements of striped  
776 bass between the exclusive economic zone and Massachusetts state waters. *N. Am. J. Fish.*  
777 *Manage.* **34**(3): 524–534. doi:10.1080/02755947.2014.892550.
- 778 Le Bris, A., Frechet, A., Galbraith, P.S., and Wroblewski, J.S. 2013a. Evidence for alternative  
779 migratory behaviours in the northern Gulf of St Lawrence population of Atlantic cod  
780 (*Gadus morhua* L.). *ICES J. Mar. Sci.* **70**(4): 793–804. doi:10.1093/icesjms/fst068.
- 781 Le Bris, A., Fréchet, A., and Wroblewski, J.S. 2013b. Supplementing electronic tagging  
782 with conventional tagging to redesign fishery closed areas. *Fish. Res.* **148**: 106–116. doi:  
783 10.1016/j.fishres.2013.08.013.
- 784 Loehrke, J.L. 2013. Movement patterns of Atlantic cod (*Gadus morhua*) spawning groups  
785 off New England. MS thesis, University of Massachusetts Dartmouth, Dartmouth, MA.
- 786 Metcalfe, J.D. and Arnold, G.P. 1997. Tracking fish with electronic tags. *Nature* **387**(6634):  
787 665–666. doi:10.1038/42622.
- 788 Moser, J. and Shepherd, G.R. 2009. Seasonal distribution and movement of black sea bass  
789 (*Centropristis striata*) in the northwest Atlantic as determined from a mark-recapture  
790 experiment. *J. Northwest Atl. Fish. Sci.* **40**: 17–28.
- 791 NECOFS 2013. Northeast Coastal Ocean Forecasting System (NECOFS) Main Portal [http:](http://fvcom.smast.umassd.edu/necofs/)  
792 [//fvcom.smast.umassd.edu/necofs/](http://fvcom.smast.umassd.edu/necofs/). Accessed: 2016-05-20.
- 793 NEFSC 2013. 55th Northeast Regional Stock Assessment Workshop (55th SAW) Assess-  
794 ment Report. Technical report, Northeast Fisheries Science Center. US Dept Com-

795 mer, Northeast Fish Sci Cent Ref Doc. 13-11; 845 p. Available from: National Ma-  
796 rine Fisheries Service, 166 Water Street, Woods Hole, MA 02543-1026, or online at  
797 <http://www.nefsc.noaa.gov/nefsc/publications/>.

798 Neuenfeldt, S., Hinrichsen, H.H., Nielsen, A., and Andersen, K. 2007. Reconstructing mi-  
799 grations of individual cod (*Gadus morhua* L.) in the Baltic Sea by using electronic data  
800 storage tags. *Fish. Oceanogr.* **16**(6): 526–535.

801 O’Donncha, F., Hartnett, M., Nash, S., Ren, L., and Ragnoli, E. 2015. Characterizing ob-  
802 served circulation patterns within a bay using HF radar and numerical model simulations.  
803 *Journal of Marine Systems* **142**: 96–110. doi:10.1016/j.jmarsys.2014.10.004.

804 Patterson, T., Thomas, L., Wilcox, C., Ovaskainen, O., and Matthiopoulos, J. 2008.  
805 State–space models of individual animal movement. *Trends Ecol. Evol.* **23**(2): 87–94.  
806 doi:10.1016/j.tree.2007.10.009.

807 Patterson, T.A., Basson, M., Bravington, M.V., and Gunn, J.S. 2009. Classifying movement  
808 behaviour in relation to environmental conditions using hidden Markov models. *J. Anim.*  
809 *Ecol.* **78**(6): 1113–1123. doi:10.1111/j.1365-2656.2009.01583.x.

810 Patterson, T.A., Parton, A., Langrock, R., Blackwell, P.G., Thomas, L., and King, R. 2016.  
811 Statistical modelling of animal movement: a myopic review and a discussion of good  
812 practice. pre-print ArXiv:1603.07511 [q-bio, stat].

813 Pedersen, M.W. 2008. HMM Geolocation Toolbox homepage [http://mwpedersen.dk/](http://mwpedersen.dk/tracking.html)  
814 [tracking.html](http://mwpedersen.dk/tracking.html). Accessed: 2016-05-20.

- 815 Pedersen, M.W., Patterson, T.A., Thygesen, U.H., and Madsen, H. 2011a. Estimating  
816 animal behavior and residency from movement data. *Oikos* **120**(9): 1281–1290. doi:  
817 10.1111/j.1600-0706.2011.19044.x.
- 818 Pedersen, M.W., Righton, D., Thygesen, U.H., Andersen, K.H., and Madsen, H. 2008. Ge-  
819 olocation of North Sea cod (*Gadus morhua*) using hidden Markov models and behavioural  
820 switching. *Can. J. Fish. Aquat. Sci.* **65**(11): 2367–2377.
- 821 Pedersen, M.W. 2007. Hidden Markov models for geolocation of fish. Ph.D. thesis, Technical  
822 University of Denmark, DTU, DK-2800 Kgs. Lyngby, Denmark.
- 823 Pedersen, M., Thygesen, U., and Madsen, H. 2011b. Nonlinear tracking in a diffusion process  
824 with a Bayesian filter and the finite element method. *Computational Statistics & Data*  
825 *Analysis* **55**(1): 280–290. doi:10.1016/j.csda.2010.04.018.
- 826 Potemra, J.T. 2012. Numerical modeling with application to tracking marine debris. *Mar.*  
827 *Pollut. Bull.* **65**(13): 42–50. doi:10.1016/j.marpolbul.2011.06.026.
- 828 Righton, D. and Mills, C. 2008. Reconstructing the movements of free-ranging demersal fish  
829 in the North Sea: a data-matching and simulation method. *Mar. Biol.* **153**(4): 507–521.  
830 doi:10.1007/s00227-007-0818-6.
- 831 Sibert, J.R., Hampton, J., Fournier, D.A., and Bills, P.J. 1999. An advec-  
832 tion–diffusion–reaction model for the estimation of fish movement parameters from tagging  
833 data, with application to skipjack tuna (*Katsuwonus pelamis*). *Can. J. Fish. Aquat. Sci.*  
834 **56**(6): 925–938. doi:10.1139/f99-017.

835 Tallack, S.M. 2011. Stock identification applications of conventional tagging data for Atlantic  
836 cod in the Gulf of Maine. In American Fisheries Society Symposium, volume 76. volume 76,  
837 pp. 1–15.

838 Teo, S.L., Boustany, A., Blackwell, S., Walli, A., Weng, K.C., and Block, B.A. 2004. Val-  
839 idation of geolocation estimates based on light level and sea surface temperature from  
840 electronic tags. *Mar. Ecol. Prog. Ser.* **283**: 81–98.

841 Thorsteinsson, V., Pálsson, O.K., Tómasson, G.G., Jónsdóttir, I.G., and Pampoulie, C.  
842 2012. Consistency in the behaviour types of the Atlantic cod: repeatability, timing of  
843 migration and geo-location. *Mar. Ecol. Prog. Ser.* **462**: 251–260. doi:10.3354/meps09852.

844 Thygesen, U.H. and Nielsen, A. 2009. Lessons from a Prototype Geolocation Problem. In  
845 Tagging and Tracking of Marine Animals with Electronic Devices, edited by J.L. Nielsen,  
846 H. Arrizabalaga, N. Fragoso, A. Hobday, M. Lutcavage, and J. Sibert, Springer Nether-  
847 lands, number 9 in Reviews: Methods and Technologies in Fish Biology and Fisheries, pp.  
848 257–276.

849 Thygesen, U.H., Pedersen, M.W., and Madsen, H. 2009. Geolocating fish using hidden  
850 Markov models and data storage tags. In Tagging and Tracking of Marine Animals  
851 with Electronic Devices, edited by J.L. Nielsen, H. Arrizabalaga, N. Fragoso, A. Hob-  
852 day, M. Lutcavage, and J. Sibert, Springer Netherlands, number 9 in Reviews: Methods  
853 and Technologies in Fish Biology and Fisheries, pp. 277–293.

854 Trauth, M., Gebbers, R., Sillmann, E., and Marwan, N. 2007. MATLAB® Recipes for Earth  
855 Sciences. Springer Berlin Heidelberg.

856 Twomey, E. and Signell, R. 2013. Construction of a 3-arcsecond digital elevation model  
857 for the Gulf of Maine. Technical Open-File Report 2011-1127, U.S. Geological Survey.  
858 <http://pubs.usgs.gov/of/2011/1127/>.

859 Warner, J.C., Geyer, W.R., and Lerczak, J.A. 2005. Numerical modeling of an estuary:  
860 A comprehensive skill assessment. *J. Geophys. Res.* **110**(C5): C05001. doi:10.1029/  
861 2004JC002691.

862 Wilkin, J.L. 2006. The summertime heat budget and circulation of southeast New England  
863 shelf waters. *Journal of Physical Oceanography* **36**(11): 1997–2011. doi:10.1175/JPO2968.  
864 1.

865 Willmott, C.J. 1981. On the validation of models. *Physical Geography* **2**(2): 184–194.  
866 doi:10.1080/02723646.1981.10642213.

867 Winship, A.J., Jorgensen, S.J., Shaffer, S.A., Jonsen, I.D., Robinson, P.W., Costa, D.P.,  
868 and Block, B.A. 2012. State-space framework for estimating measurement error from  
869 double-tagging telemetry experiments. *Methods Ecol. Evol.* **3**(2): 291–302. doi:10.1111/  
870 j.2041-210X.2011.00161.x.

871 Woillez, M., Fablet, R., Ngo, T.T., Lalire, M., Lazure, P., and de Pontual, H. 2016. A  
872 HMM-based model to geolocate pelagic fish from high-resolution individual temperature  
873 and depth histories: European sea bass as a case study. *Ecol. Model.* **321**: 10–22. doi:  
874 10.1016/j.ecolmodel.2015.10.024.

875 Wright, P.J., Neat, F.C., Gibb, F.M., Gibb, I.M., and Thordarson, H. 2006. Evidence for

876 metapopulation structuring in cod from the west of Scotland and North Sea. *J. Fish Biol.*  
877 **69**: 181–199. doi:10.1111/j.1095-8649.2006.01262.x.

878 Zemeckis, D.R., Hoffman, W.S., Dean, M.J., Armstrong, M.P., and Cadrin, S.X. 2014a.  
879 Spawning site fidelity by Atlantic cod (*Gadus morhua*) in the Gulf of Maine: implications  
880 for population structure and rebuilding. *ICES J. Mar. Sci.* doi:10.1093/icesjms/fsu117.

881 Zemeckis, D.R., Martins, D., Kerr, L.A., and Cadrin, S.X. 2014b. Stock identification of  
882 Atlantic cod (*Gadus morhua*) in US waters: an interdisciplinary approach. *ICES J. Mar.*  
883 *Sci.* **71**(6): 1490–1506. doi:10.1093/icesjms/fsu032.

884 Zemeckis, D., Liu, C., Cowles, G., Dean, M., Hoffman, W., Martins, D., and Cadrin, S.  
885 2017. Seasonal movements and connectivity of an Atlantic cod *Gadus morhua* spawning  
886 component in the western Gulf of Maine. *ICES J. Mar. Sci.* doi:10.1093/icesjms/fsw190.

887 Zemeckis, D.R. 2016. Spawning dynamics, seasonal movements, and population structure  
888 of Atlantic cod (*Gadus morhua*) in the Gulf of Maine. PhD thesis, University of Mas-  
889 sachusetts Dartmouth, Dartmouth, MA.

## Figure captions

- 890 **Figure captions**
- 891 Figure 1 (a) Model domain, horizontal mesh, and bathymetry (m) of the North-  
892 east Coastal Ocean Forecasting System (NECOFS). (b) Map of west-  
893 ern Gulf of Maine, with the acoustic receiver arrays (inset) deployed  
894 within the Spring Cod Conservation Zone
- 895 Figure 2 Examples of the three activity levels identified in data from the  
896 archival data storage tags using the tidal fitting algorithm: a) low  
897 activity, b) moderate activity, and c) high activity. The shaded areas  
898 represent the 13 h window used to identify low activity periods and  
899 the 5 h window used to identify moderate activity periods.
- 900 Figure 3 Example of the likelihood functions based on temperature and depth  
901  $[L_{dt}(\hat{\mathbf{x}})]$  and modified with tidal exclusion  $[L(\hat{\mathbf{x}})]$  for a given day.
- 902 Figure 4 Example of simulated tracks in the Gulf of Maine (GoM) and Georges  
903 Bank (GB) with duration of 40 (yellow), 120 (yellow and red), and  
904 360 (yellow, red, and blue) days.
- 905 Figure 5 Areas of daily 95% utilization distribution determined from acoustic  
906 array detection of the high, moderate, and low activity levels deter-  
907 mined by the likelihood model. Box plots show median values (red  
908 horizontal line), 25% and 75% percentile values (box outline), and  
909 the highest and lowest value within 1.5 times the interquartile range  
910 (whiskers).

911 Figure 6 Actual (star) and estimated (dot) locations of mooring tag deploy-  
912 ments for tags a) #73; b) #84; and c) #71, in order of increasing  
913 location error.

914 Figure 7 Locations of the 10 double-electronic-tagged cod detected by the  
915 acoustic receivers (blue triangles) and the corresponding same-day  
916 estimates constructed by the revised (red dots) and original (open  
917 circles) HMM Geolocation Toolbox.

918 Figure 8 Daily location estimation error for the simulated experiments. Box  
919 plots show median values (horizontal line), 25% and 75% percentile  
920 values (box outline), outliers (diamonds), and the highest and lowest  
921 value within 1.5 times the interquartile range (whiskers).

922 Figure 9 The most probable track and the associated total posterior distribu-  
923 tion for the double-electronic-tagged cod. The Spring Cod Conserva-  
924 tion Zone (SCCZ, Fig. 1) is also shown (red rectangle).

925 Figure 10 Depth (blue line) and temperature (red line) time series recorded by  
926 DST and the activity classification (shading color, dark green: low,  
927 light green: moderate, white: high) for double-electronic-tagged cod  
928 nos. 12 and 13.

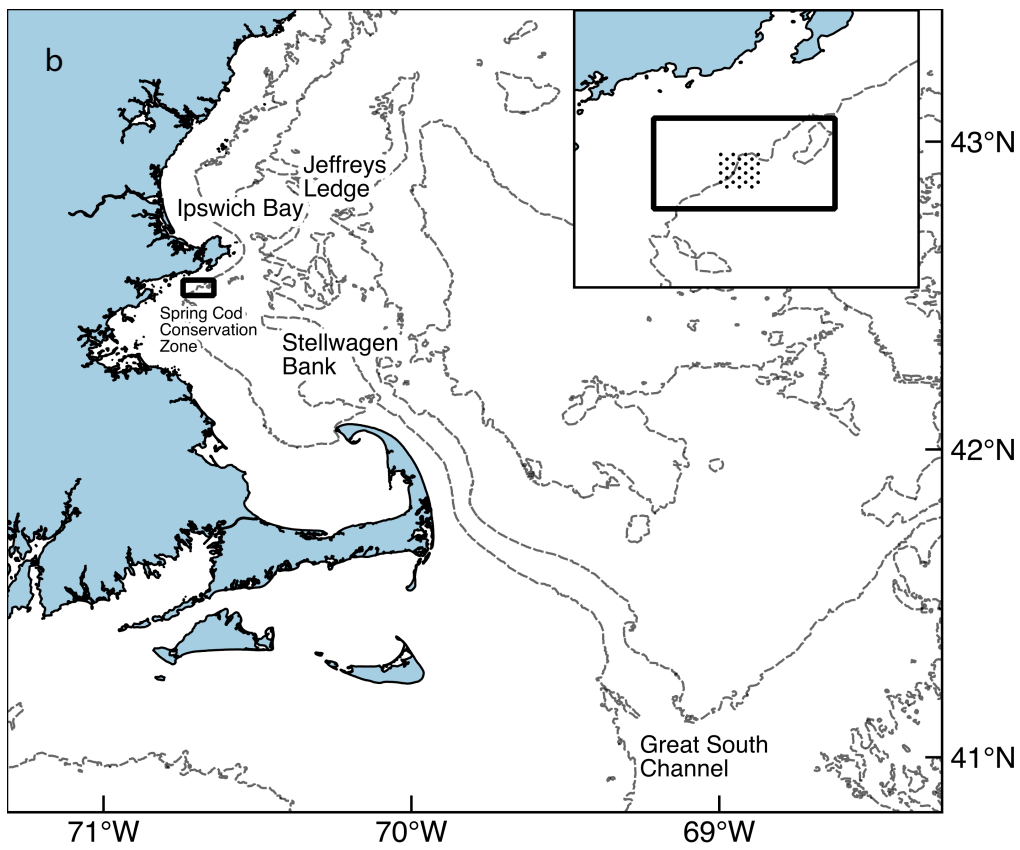
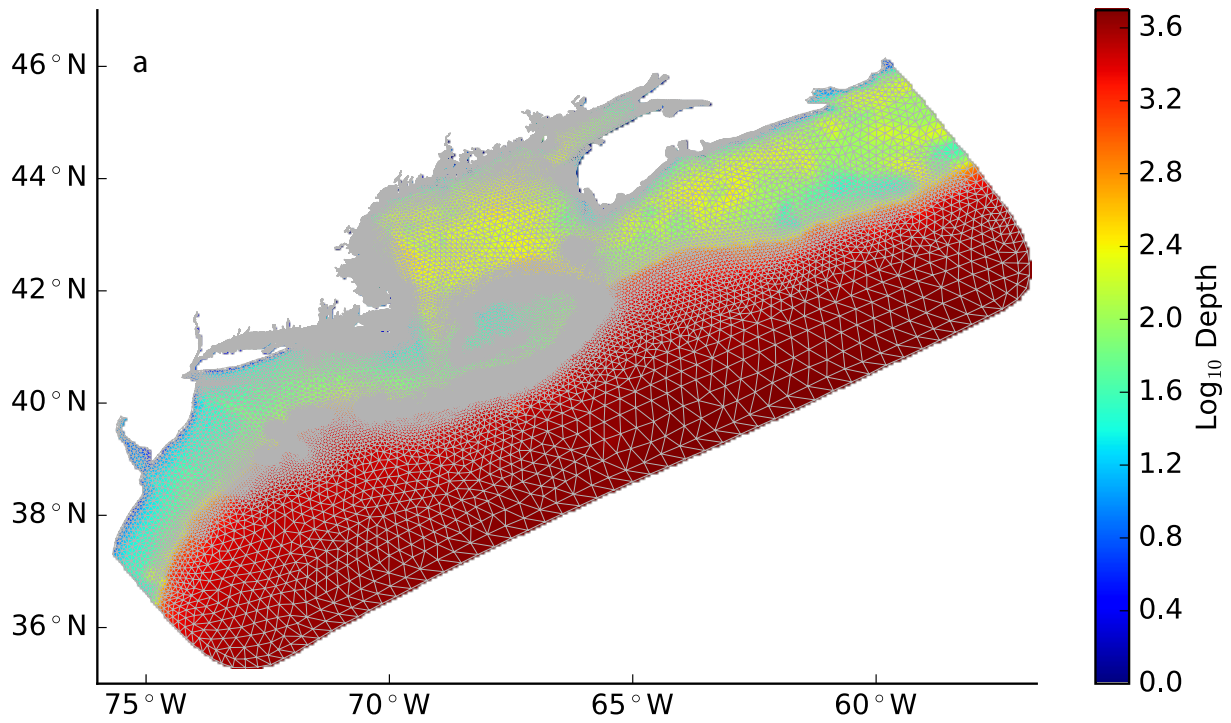


Figure 1

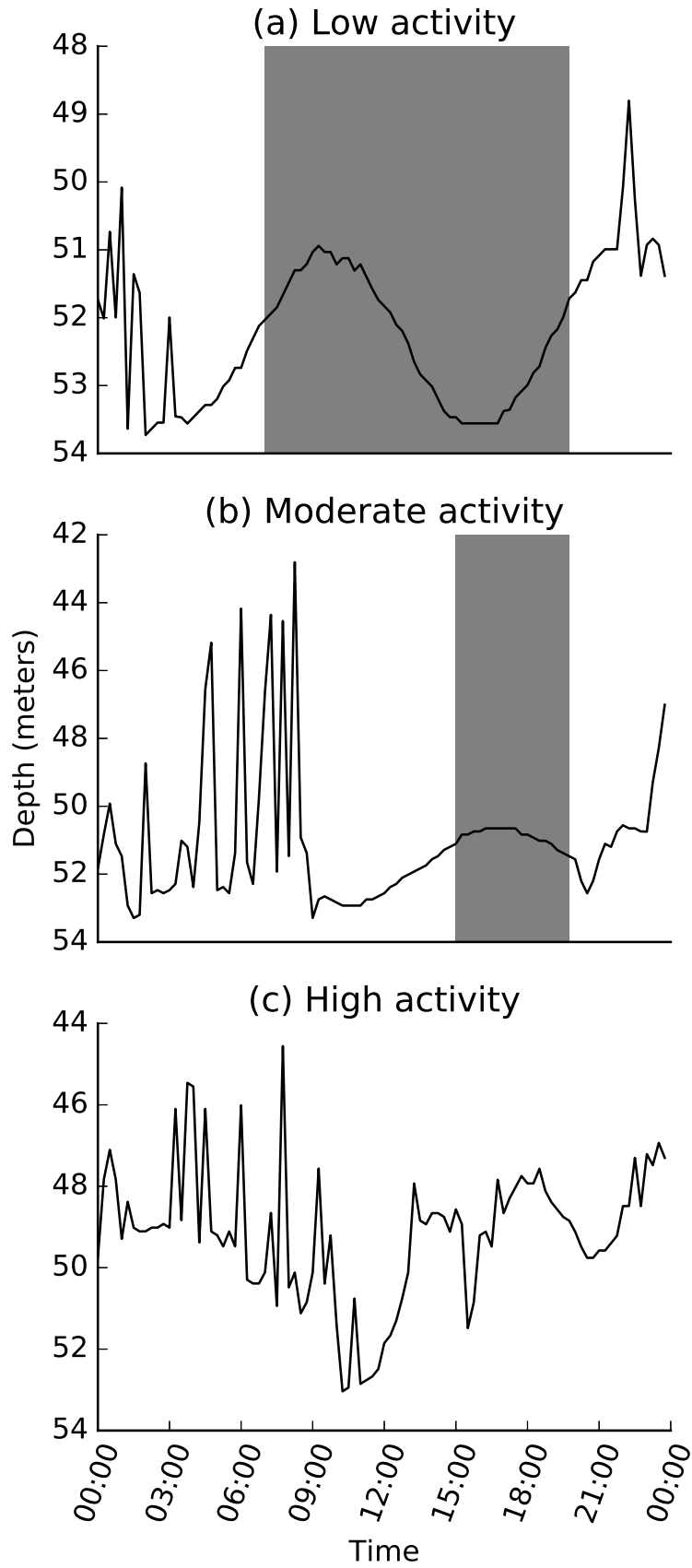


Figure 2  
47

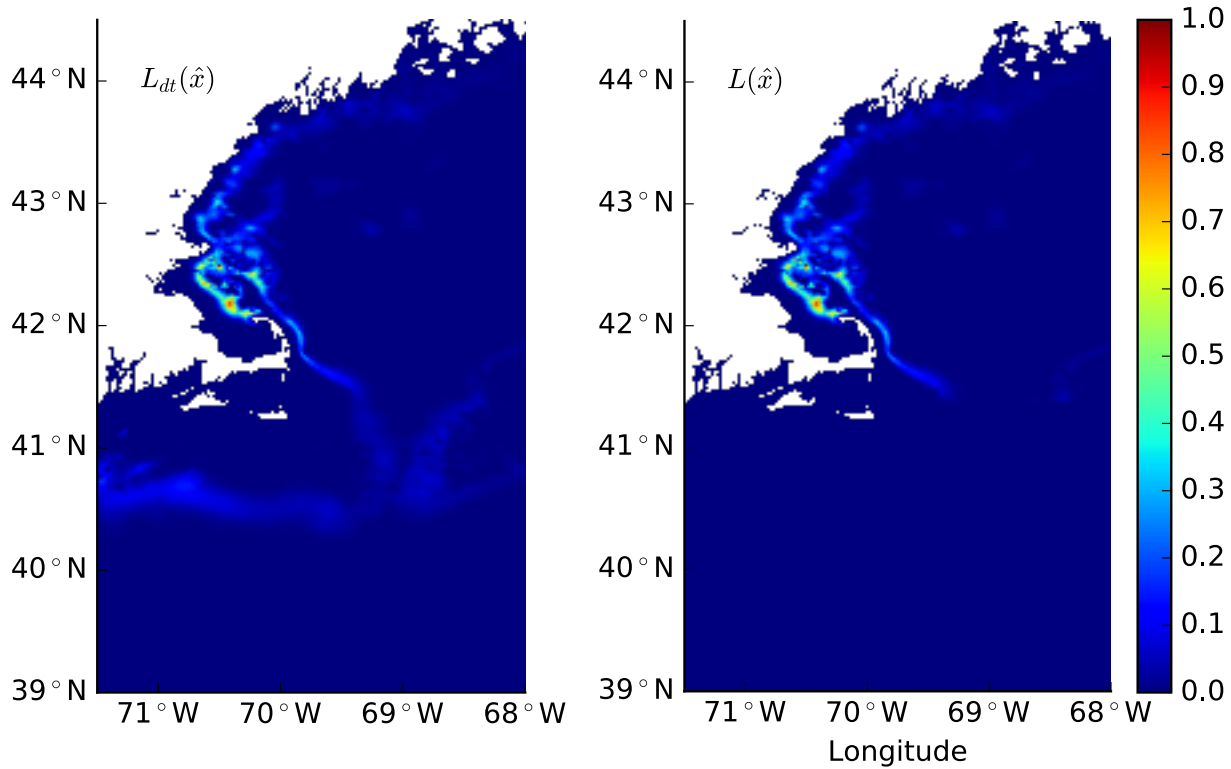


Figure 3

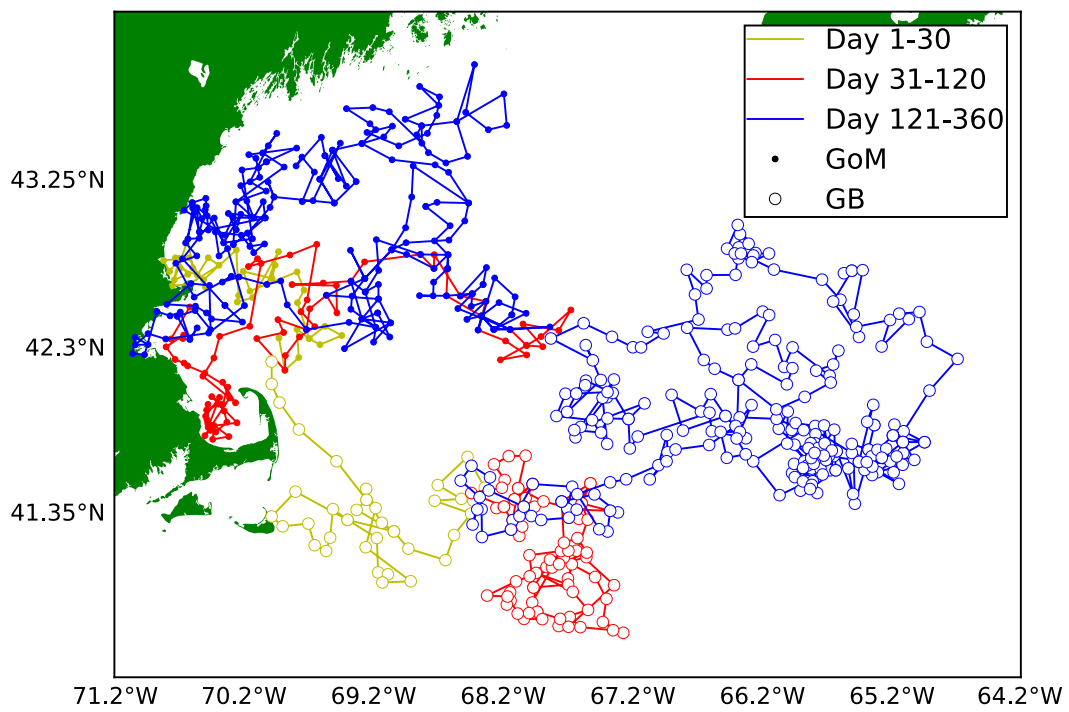


Figure 4

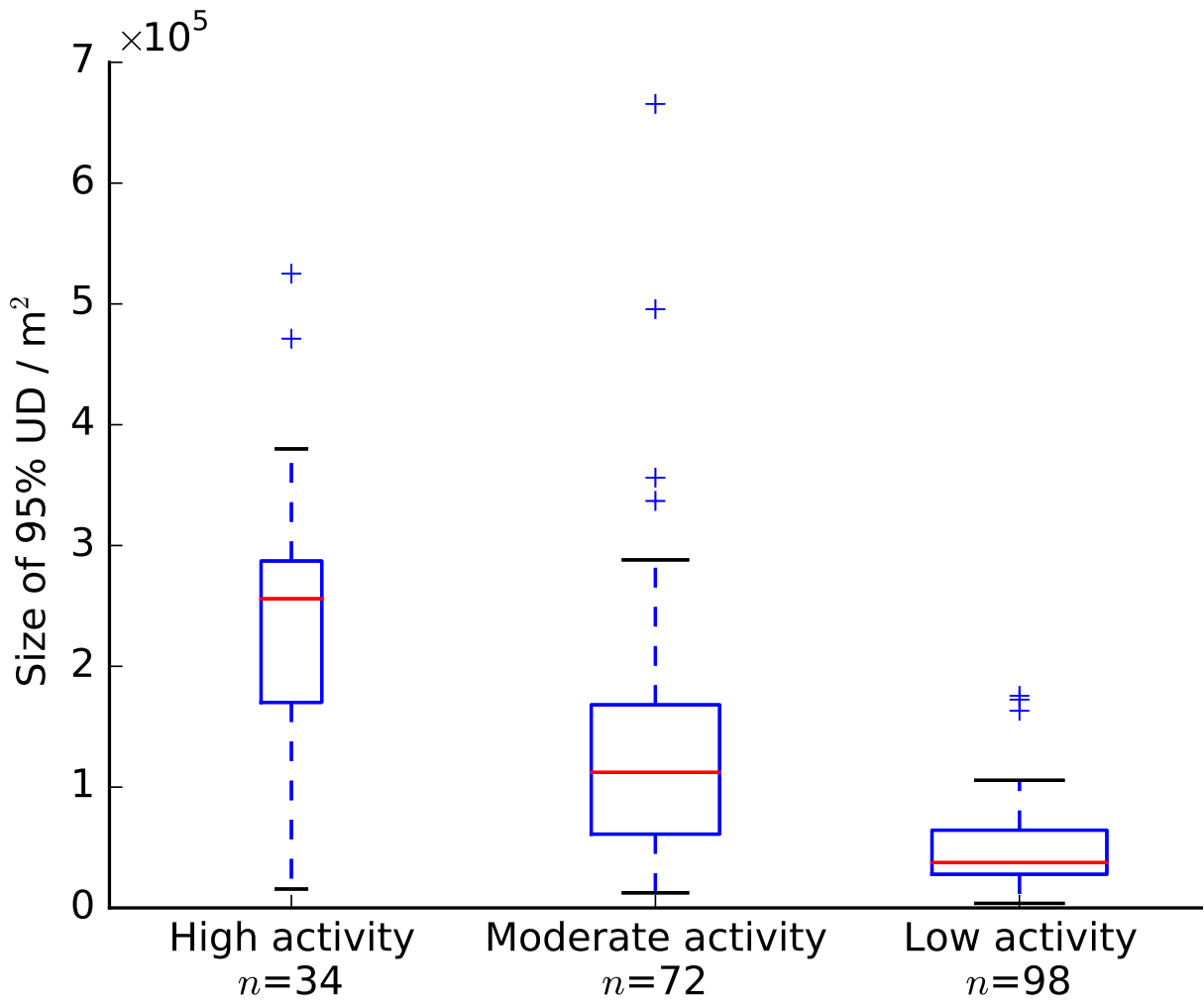


Figure 5

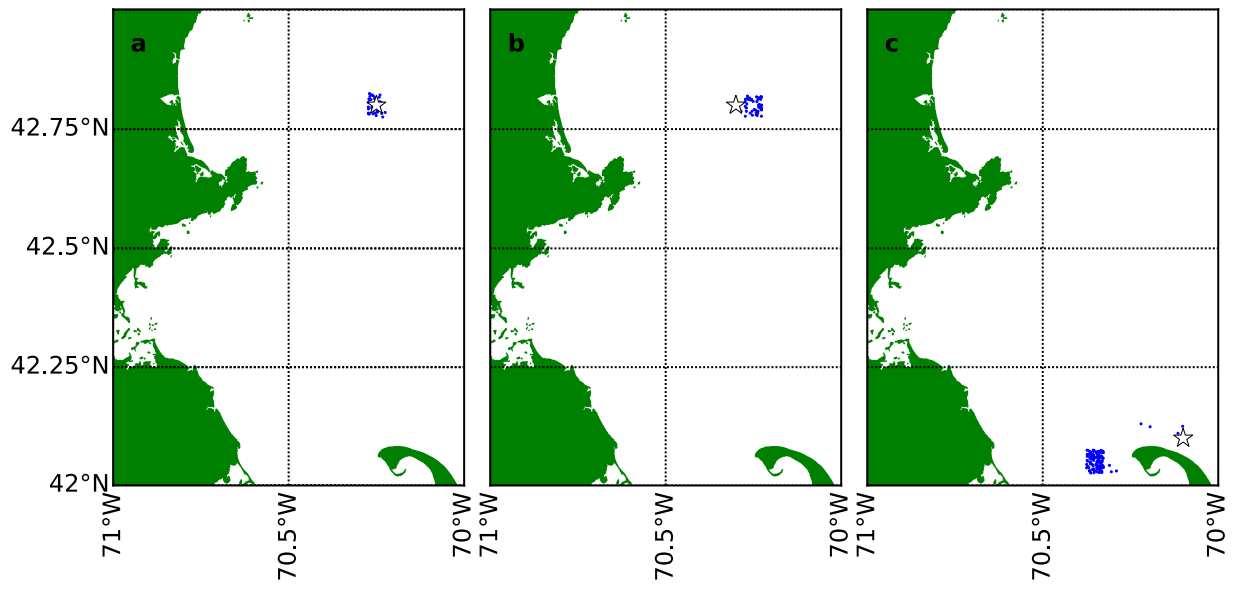


Figure 6



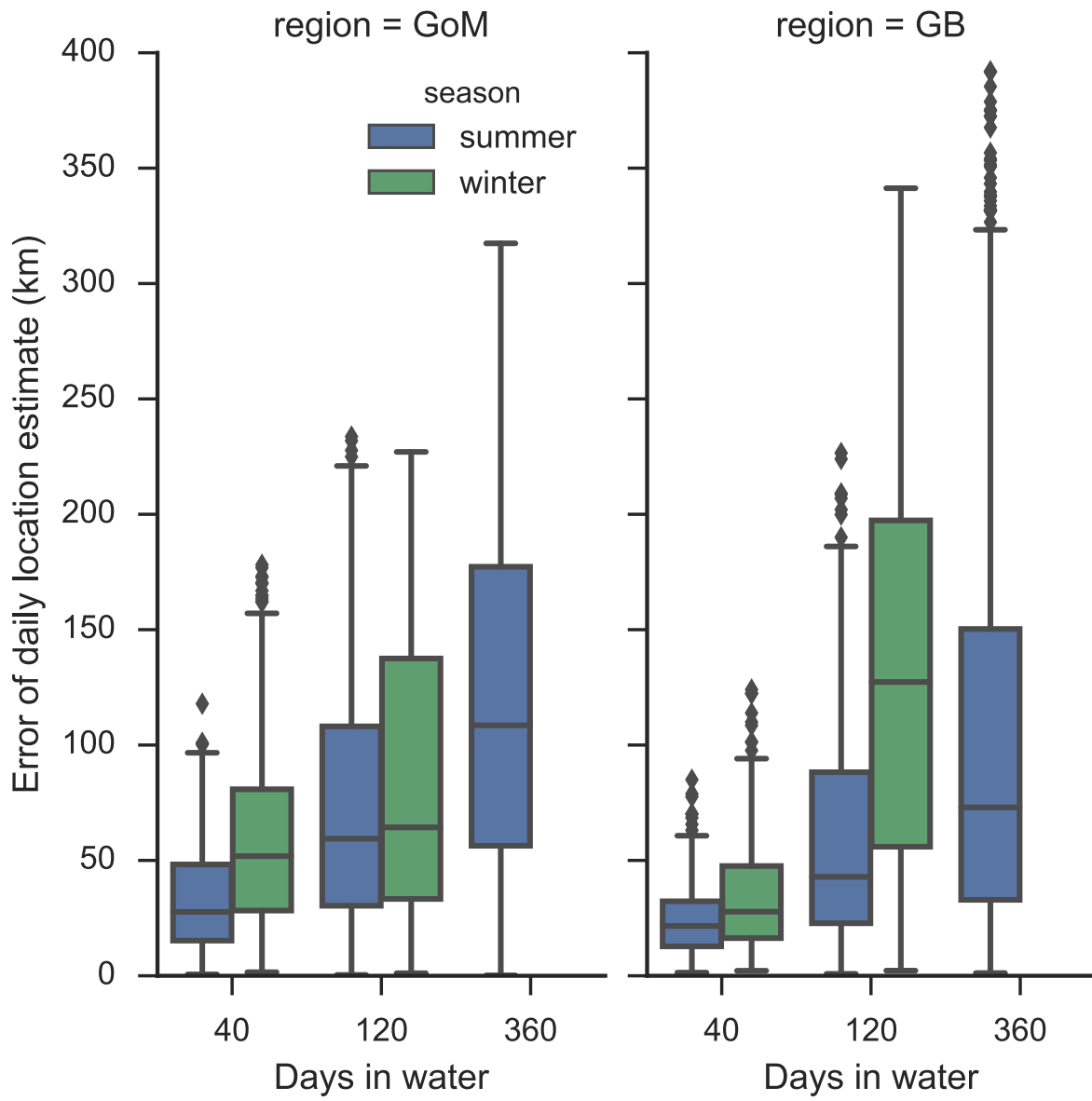


Figure 8

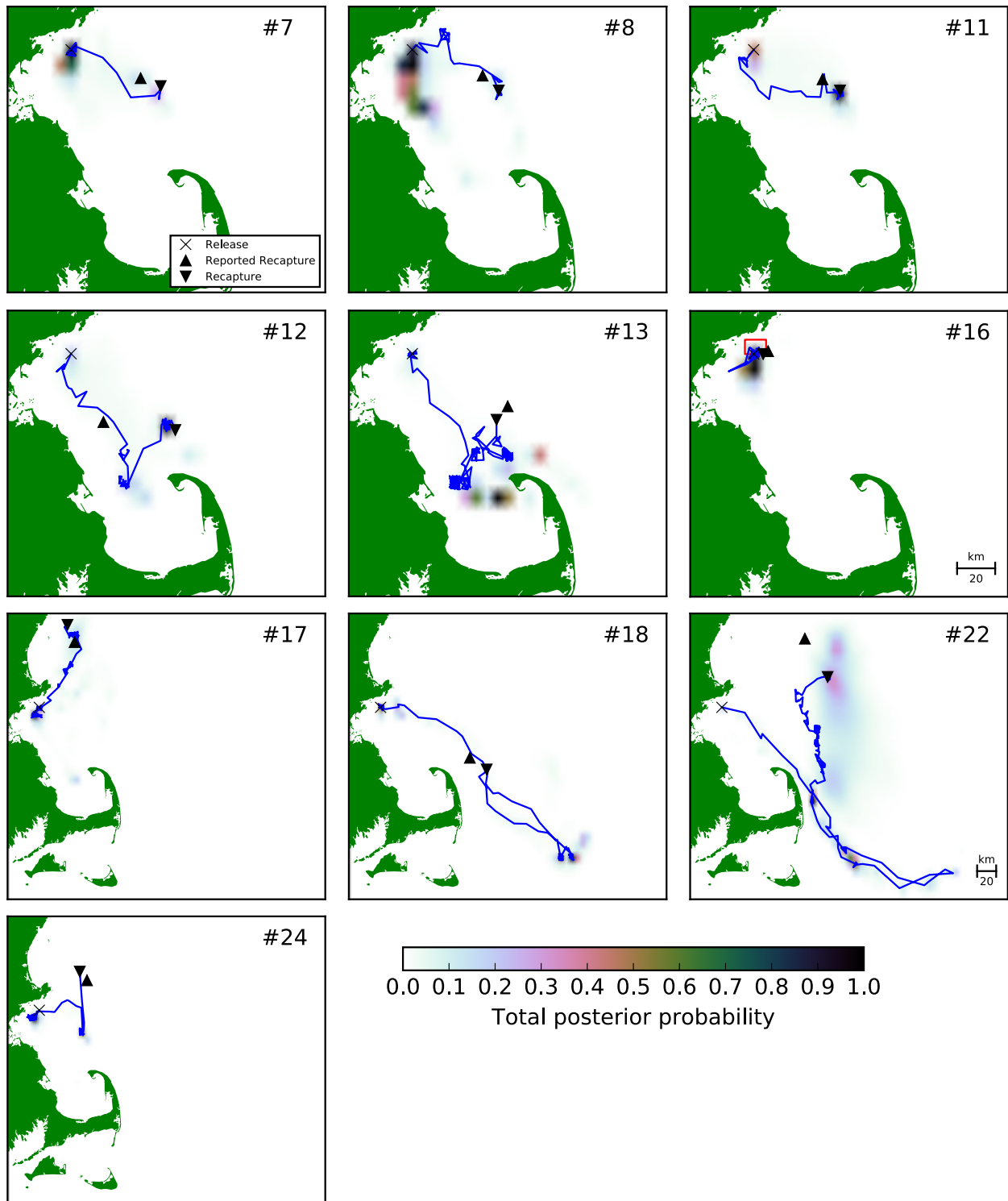


Figure 9

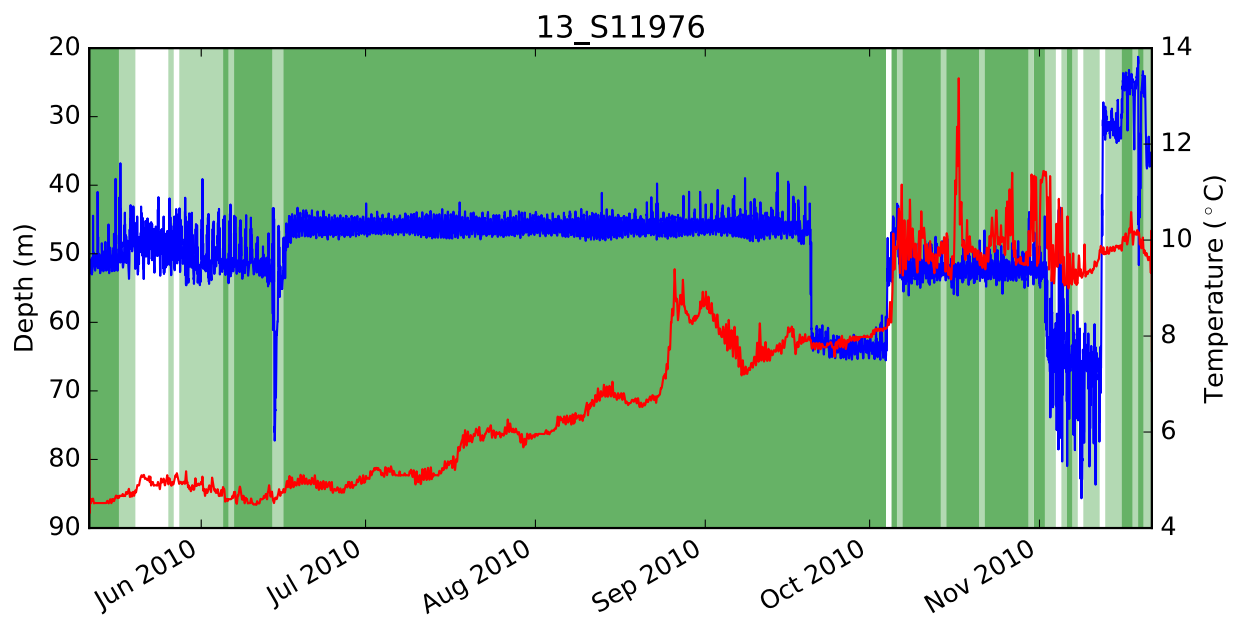
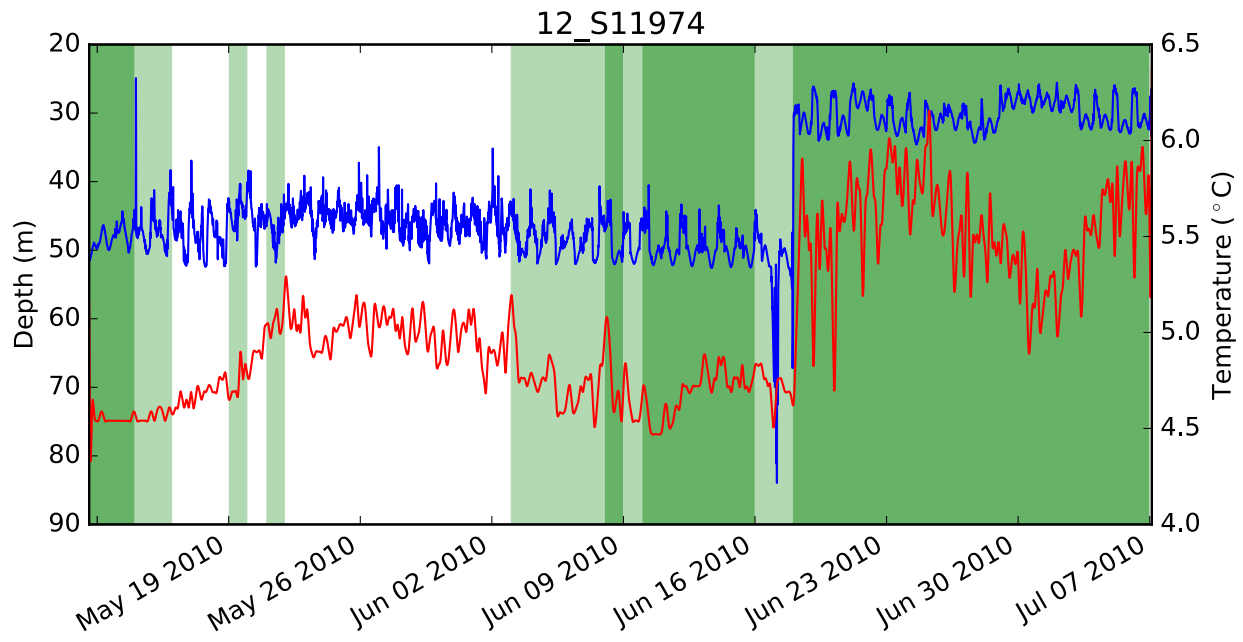


Figure 10

## 929 **Table captions**

930	Table 1	Comparisons of bottom temperature between NECOFS FVCOM pre-
931		dictions and survey measurements. NEFSC: NOAA Northeast Fish-
932		eries Science Center, MADMF: Massachusetts Division of Marine
933		Fisheries, SMAST: School for Marine Science and Technology, UMass
934		Dartmouth, IBS: Industry-Based Surveys.
935	Table 2	Experimental setup for the simulated tracks. GoM=Gulf of Maine;
936		GB=Georges Bank; Summer=Aug 10, 2012; Winter=Jan 12, 2013
937	Table 3	Validation results for mooring tags and double-electronic-tagged cod.
938	Table 4	Summary of tagging and geolocation data for 10 double-electronic-
939		tagged Atlantic cod. All tagged cod were released at 42.52° N, 70.70°
940		W. MPT: most probable track

Table 1

Survey	Time	Number of measurements	Model-observation difference (°C)				
			Mean	S.D.	RMSE	Min	Max
NEFSC Bottom Trawl Survey	2009, 2014–2015	1 478	0.13	1.79	1.80	-6.58	7.53
NEFSC Shrimp Survey	2009 – 2013	361	-0.26	0.97	1.01	-4.30	2.05
MADMF Bottom Trawl Survey	2010 – 2015	1 299	-0.21	1.72	1.73	-7.44	4.66
SMAST Study Fleet	2003 – 2007	17 009	0.14	1.37	1.38	-10.73	8.84
SMAST 2010 Winter Flounder IBS	2010	336	0.62	1.57	1.68	-4.69	5.33
SMAST 2011 Winter Flounder IBS	2011	257	0.99	3.08	3.23	-4.77	6.32
SMAST 2012 Winter Flounder IBS	2012	159	-0.99	1.33	1.66	-5.12	0.90
SMAST Cod IBS	2003 – 2007	2 310	-0.43	0.98	1.07	-5.68	2.64
SMAST Video Survey	2013 – 2015	6 292	-0.40	2.09	2.12	-7.02	7.80
Total		29 501	-0.04	1.61	1.61	-10.73	8.84

Table 2

Set	Tag No.	Region	Season of release	Duration in water (d)
1	1–5	GoM	Summer	40
2	6–10	GoM	Summer	120
3	11–15	GoM	Summer	360
4	16–20	GoM	Winter	40
5	21–25	GoM	Winter	120
6	26–30	GB	Summer	40
7	31–35	GB	Summer	120
8	36–40	GB	Summer	360
9	41–45	GB	Winter	40
10	46–50	GB	Winter	120

Table 3

Experiment	Tag/fish No.	Deployment date	Deployment location	Days of data	Error range (km)	RMSE (km)	Median (km)	SD (km)	Mean normalized probability at known location(s)
a) Stationary	63	Jun 18, 2010	42.53° N, 70.70° W	31	3.10–12.12	9.22	9.02	1.81	0.84
	64	Apr 1, 2012	42.87° N, 70.60° W	33	0.76–5.25	3.27	2.88	1.22	1.00
	65	Apr 2, 2012	42.43° N, 70.68° W	17	5.85–11.11	8.94	9.35	1.81	0.84
	66	Apr 3, 2012	42.52° N, 70.69° W	27	0.46–4.63	2.58	2.44	1.81	0.77
	67	Apr 11, 2012	42.69° N, 70.43° W	23	0.73–4.88	2.96	2.34	1.25	0.86
	71	Aug 1, 2014	42.10° N, 70.08° W	126	3.23–25.51	22.86	23.10	2.62	0.80
	72	Apr 6, 2015	42.84° N, 70.27° W	36	1.13–21.38	18.28	18.88	4.23	0.65
	73	Apr 6, 2015	42.80° N, 70.27° W	36	0.58–4.24	2.09	1.86	0.84	1.00
	81	Apr 6, 2015	42.82° N, 70.27° W	113	0.14–6.09	3.42	3.16	1.40	0.52
	82	Apr 6, 2015	42.79° N, 70.32° W	134	3.47–8.20	6.03	5.83	1.19	0.30
	83	Sep 1, 2015	42.81° N, 70.29° W	43	1.65–6.75	4.54	4.79	1.39	0.77
	84	Sep 1, 2015	42.80° N, 70.31° W	43	1.35–6.81	4.85	4.59	1.37	0.94
	85	Sep 1, 2015	42.82° N, 70.27° W	43	0.22–5.97	3.49	3.29	1.39	0.94
	86	Sep 1, 2015	42.81° N, 70.27° W	43	0.28–5.22	2.83	2.64	1.24	0.72
<b>Total</b>				<b>748</b>	<b>0.14–25.51</b>	<b>11.07</b>	<b>4.93</b>	<b>7.63</b>	<b>0.69</b>
<b>b) Stationary (total, with original HGT)</b>									
	7	May 7, 2010	42.52° N, 70.70° W	15	1.08–19.27	6.51	3.12	4.89	0.74
	8	May 7, 2010	42.52° N, 70.70° W	17	1.87–25.95	13.89	13.25	5.14	0.26
	11	May 11, 2010	42.52° N, 70.70° W	16	6.52–31.35	18.11	15.65	8.55	0.61
	12	May 11, 2010	42.52° N, 70.70° W	36	6.75–58.20	42.17	44.97	18.51	0.54
	13	May 11, 2010	42.52° N, 70.70° W	34	1.18–57.32	42.37	48.41	22.10	0.47
c) Double-electronic-tagged	16	Jun 18, 2010	42.52° N, 70.70° W	26	0.39–7.41	3.16	2.19	1.68	0.79
	17	Jun 18, 2010	42.52° N, 70.70° W	23	0.55–12.21	8.55	8.33	2.31	0.41
	18	Jun 18, 2010	42.52° N, 70.70° W	14	0.61–4.37	2.40	2.22	1.04	0.39
	22	Jul 7, 2010	42.52° N, 70.70° W	8	18.28–134.38	97.44	91.45	43.53	0.34
	24	May 20, 2011	42.52° N, 70.70° W	35	6.11–12.87	8.95	8.85	1.75	0.83
	<b>Total</b>				<b>223</b>	<b>0.38–97.27</b>	<b>21.87</b>	<b>6.45</b>	<b>16.69</b>
<b>d) Double-electronic-tagged (total, with original HGT)</b>									
				<b>223</b>	<b>0.59–51.70</b>	<b>32.76</b>	<b>34.80</b>	<b>15.43</b>	<b>0.06</b>

Table 4

Fish No.	DMF Fish ID	Tag No.	Release Date	Recapture		Days at large	Displacement distance (km)	Length of estimated movement (MPT, km)	Error of estimated recapture location (km)	# days of low activity	# days of moderate activity	Average movement rate (km/day)	
				Date	Uncertainty (km)								Latitude (°)
7	156	S11951	May 7, 2010	May 26, 2010	42.40 N	70.37 W	15	29.28	87.93	8.38	11	7	4.63
8	157	S11938	May 7, 2010	Jun 4, 2010	42.41 N	70.37 W	15	29.09	112.15	8.52	18	5	4.01
11	173	S11971	May 11, 2010	Jun 8, 2010	42.40 N	70.38 W	15	29.07	111.94	8.09	17	4	4.00
12	172	S11974	May 11, 2010	Jul 6, 2010	42.26 N	70.55 W	30	30.97	208.16	28.18	29	12	3.72
13	175	S11976	May 11, 2010	Nov 21, 2010	42.32 N	70.25 W	15	42.47	586.87	6.80	152	32	3.03
16	229	S12060	Jun 18, 2010	Jul 15, 2010	42.51 N	70.63 W	15	4.97	86.48	2.22	18	9	3.20
17	230	S12061	Jun 18, 2010	Aug 29, 2010	42.95 N	70.37 W	15	55.16	276.52	14.25	27	33	3.84
18	231	S12059	Jun 18, 2010	Sep 18, 2010	42.15 N	69.86 W	15	80.62	487.52	16.00	44	33	5.30
22	242	S12068	Jul 7, 2010	Feb 4, 2011	42.98 N	69.92 W	30	81.07	974.48	34.33	24	42	4.60
24	282	S11845	May 20, 2011	Jul 26, 2011	42.71 N	70.25 W	15	41.87	274.96	8.68	45	18	4.10